Simulator Evaluations of Higher Automation Autoflight Concepts for Various eVTOL Vehicle Configurations

Thomas Lombaerts* Kimberlee Shish† John Kaneshige‡ Amber Villa§ Michael Feary¶ Kevin Monk‖ Sandy Lozito**
Loran Haworth†† Mieczysław Steglíński‡‡ Elif Kürklü§§ Nelson Iwai¶¶ John Archdeacon*** Barth Baron †††
NASA Ames Research Center, Moffett Field, CA 94035

Electric Vertical Takeoff and Landing vehicles have the potential to unlock a new concept of urban mobility through the air but also introduce multiple challenges on how to integrate these revolutionary vehicles into the existing airspace with its various users. One mid-term airspace concept proposes integrating eVTOL aircraft at scale into complex, high-tempo airspace with diverse aircraft types through the development of new procedures, routes, communication protocols and cooperative airspace constructs including corridors. This paper presents simulator evaluations of proposed Urban Air Mobility (UAM) operations and procedure concepts to examine efficacy of the operations from the perspective of pilots flying. Nine pilots were recruited to fly three dissimiliar, yet industry representative eVTOL aircraft designs with shared automation and control interfaces in the Vertical Motion Simulator at NASA Ames Research Center. Scenarios were designed to explore new airspace operation concepts including interactions with mixed-equipage traffic such as legacy transport traffic and other eVTOL traffic. Higher automation functionality is developed to meet the defined operational requirements, including a simplified vehicle command concept with assistive hover, autopilot and flight management capabilities. Results indicate that the higher precision navigational and temporal constraints were achievable with sufficient automation and identify some challenges associated with designing airspace procedures and operational concepts that serve a diversity of aircraft performance characteristics.

I. Introduction

Urban Air Mobility (UAM) has the potential to unlock a whole new concept of urban mobility through the air, but requires integration in the existing airspace with its various users. One approach to integrating electric Vertical Takeoff and Landing (eVTOL) vehicles into existing airspace operations at scale (higher tempo) proposes the use of defined cooperative areas (corridors) and federated extensible air traffic management services, including the use of a Provider of Services for UAM (PSU) to support cooperative management of UAM traffic [1]. Airspace designs have developed cooperative areas when operating through class B with defined coordination and communication protocols [2, 3]. PSU services designed to meet Demand Capacity Balancing (DCB) and Sequencing and Scheduling constraints support

*Aerospace Research Engineer, KBR, Intelligent Systems Division, Mail Stop 269-1, AIAA Associate Fellow, email: thomas.lombaerts@nasa.gov.
†Aerospace Engineer, NASA Ames Research Center, Intelligent Systems Division, Mail Stop 269-1, AIAA member, email: kimberlee.h.shish@nasa.gov.
‡Computer Engineer, NASA Ames Research Center, Intelligent Systems Division, Mail Stop 269-1, AIAA member, email: john.t.kaneshige@nasa.gov.
§Aerospace Engineer, NASA Ames Research Center, Human Systems Integration Division, Mail Stop 262-1, email: amber.n.villa@nasa.gov.
¶Aerospace Technologist, NASA Ames Research Center, Human Systems Integration Division, Mail Stop 262-1, AIAA member, email: michael.s.feary@nasa.gov.
‖Research Engineer, NASA Ames Research Center, Human Systems Integration Division, Mail Stop 262-1, email: kevin.j.monk@nasa.gov.
**Human Factors Researcher, NASA Ames Research Center, Intelligent System Division, Mail Stop 269-1, email: sandra.c.lozito@nasa.gov.
††Consultant, San José State University Research Foundation, Human Systems Integration Division, Mail Stop 262-1, email: loran.a.haworth@nasa.gov.
‡‡Consultant, KBR, Intelligent Systems Division, Mail Stop 269-1, email: mieczyslaw.steglinski@nasa.gov.
§§Computer Scientist, KBR, Intelligent Systems Division, Mail Stop 269-1, email: elif.kurklu@nasa.gov.
¶¶Senior Principal Systems Engineer, ASRC Federal Data Solutions LLC, Human Systems Integration Division, Mail Stop 262-1, email: nelson.iwai@nasa.gov.
***Senior Principal Systems Engineer, ASRC Federal Data Solutions LLC, Human Systems Integration Division, Mail Stop 262-1, email: john.archdeacon@nasa.gov.
†††Consultant, San José State University Research Foundation, Human Systems Integration Division, Mail Stop 262-1, email: barth.a.baronjr@nasa.gov.

deconfliction of UAM operations within dense airspaces through strategically scheduling flights pre-departure with the aim of keeping operations below capacity constraints and with sufficient spacing (time) at merging points and vertiports [4, 5]. To meet the requirements to operate within this airspace concept pilots and aircraft will be expected to meet 4D trajectory constraints, conforming to their submitted operational intent. For operations in class B, tightly defined corridors can ease integration with legacy traffic by separating the operations with defined procedures. This successful integration depends on the precision that is achievable by the electric Vertical Takeoff and Landing (eVTOL) vehicles in their respective airways. A higher automation autoflight concept, consisting of a suite of enabling technologies, is an important contribution to achieve this required precision.

The goal of this experiment was to investigate the potential role of and impact of automation on eVTOL aircraft operations under a mid-term extensible Traffic Management (xTM) airspace concept [6]. The objectives are twofold. The first one is to evaluate automation enabled pilot/vehicle performance in a mission representative use case. The second objective is to analyze 4D trajectory conformance requirements and provide airspace design recommendations for enabling safe and efficient xTM operations. The set of conformance requirements and the airspace design that served as a starting point for the second objective are based on the ATM Interoperability Study (AIS) as discussed in Ref. [2].

The approach consists of the following steps. First, a representative set of automation technologies was developed for enabling eVTOL autopilot and 4D flight management capabilities. These technologies were integrated across three unique eVTOL vehicle design concepts developed by the NASA Revolutionary Vertical Lift Technologies (RVLT) project. Thereafter, UAM-specific operating procedures and an operational concept were derived from the ATM Interoperability Study (AIS) Letter of Agreement (LoA) [2]. Consequently, a navigational database and corresponding charts were constructed based on the Dallas 2040 Adaptation (based on a snapshot taken on October 24, 2024). This paper focuses mainly on the tests using several industry representative eVTOL vehicle design concepts and their performance in the Vertical Motion Simulator (VMS).

This work fits in the Pilot Automation Interaction (PAI) framework, and is part of a larger scale research effort spanning over multiple years that explores multiple PAI Control Automation Levels. Previous work focused on lower levels of automation with stability augmented control, where different control concepts were explored as discussed in [7], as well as different Assistive Hover Automation (AHA) strategies, presented in [8, 9].

II. Development of Materials

A. Airspace Design

A mid-term use case for an airspace concept was constructed based on the Dallas 2040 Adaptation. This adaptation is based on an ATM Interoperability Study (AIS) that was conducted in 2024 [2]. Key takeaways from this study are threefold. First of all, corridors were defined as cooperative areas through class B airspace that allow separation of UAM aircraft from legacy traffic. Secondly, a Letter of Agreement (LOA) defines operations, routes and coordination points. Finally, this study evaluated ATC workload and acceptability of these aforementioned UAM corridors.

Figure 1 shows the various vertiports and the aforementioned UAM corridors in the context of the Dallas 2040 Adaptation. Two vertiports are located at Dallas Love Field (DAL): DF60 on the business jets ramp and DF61 on the rooftop of a parking garage between the two runways. Another vertiport (DF49) is located in downtown Dallas and the DF120 vertiport is located in Terminal E of Dallas-Fort Worth International Airport (DFW). All other vertiports are located in the suburban areas around Dallas-Fort Worth including DF99 located in Frisco, north of DAL. This study focuses on the route departing from DF99 through the corridor arrival to the DF60 and DF61 vertiports at DAL. This third Automation Enabled Pilot study (AEP-3) is intended to provide a flightdeck centric perspective of a near to mid-term xTM-ATM airspace concept as a first step towards a follow on study focused on the airspace perspective known as Technical Challenge Level 1 (TCL-1).

The AEP-3 aircraft operational baseline and flight plan assume that the aircraft will execute UAM-specific operating procedures, which are derived from the AIS Letter of Agreement and operational concept. These shall include the following steps:

- File and maintain an "Instrument Flight Rule (IFR)-like" flight plan within the 4D compliance specifications (while able), that is approved by the Provider of Services for UAM (PSU). It is also assumed that the PSU receives automated position updates of the vehicle.
- Maintain aircraft separation according to Visual Flight Rules (VFR).
- Monitor relevant ATC/CTAF (Common Traffic Advisory Frequency) frequencies, contact ATC and request clearance prior to entering and exiting the UAM corridors inside of Class Bravo Airspace.

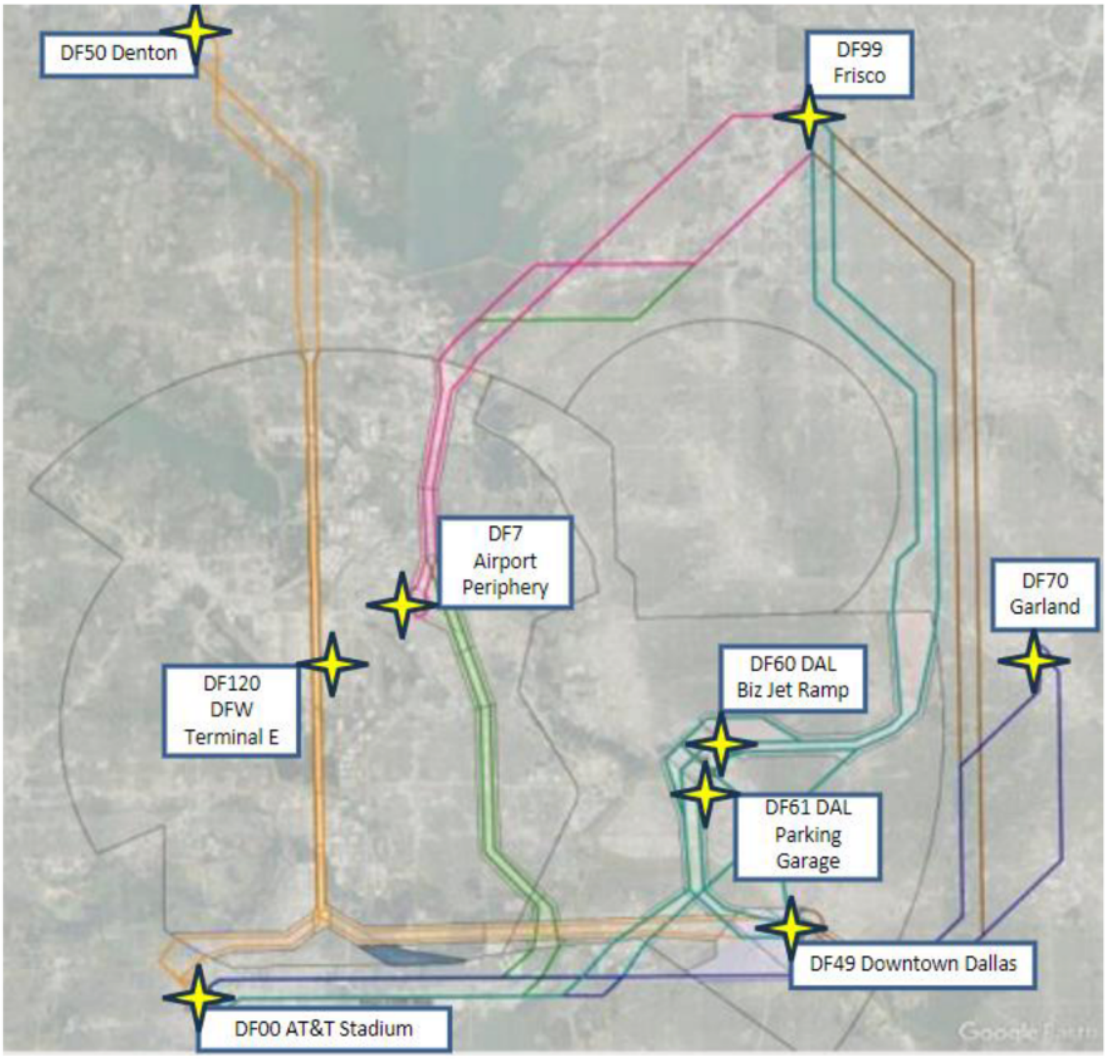


Fig. 1 UAM corridors in the Dallas 2040 Adaptation, source: [2]

Figure 2 shows the flight path and the corridors from DF99 Frisco to Dallas Love Field. The PSU assigns a scheduled departure time (STD) and a scheduled arrival time (STA) at the corridor entry, which is at waypoint EB016. The AIS LOA defines the routes and coordination points with a single file, bi-directional corridor with required navigational precision (RNP) of 0.1 nautical miles through class B airspace. Procedures and routes were implemented that were flyable and compatible with the on-board Flight Management System (FMS). The routes comprise two approaches, namely one to the signature DF60 vertipad, and one to DAL terminal DF61. Each has 3 approach transitions, namely via waypoints APEST (approach East, overflying the runway threshold), MDEST (mid East, overflying the runway) and MARSH. Coded Instrument Flight Procedures (CIFP) were developed including RF (radius to fix) legs, with a 6 degrees approach path, and also with alternate landing pads.

Figure 3 focuses on AEP-3 corridor operations into DAL, together with communications and contingencies. Waypoint EB016 serves as the point of entry into the corridor and as the pre-departure STA location. ATC clearance is required prior to corridor entry to class B airspace. There are two more reporting points in this corridor. The first one is at KELTI as shown in Fig. 3. First the pilot reports to KDAL-Approach and then is instructed to switch to KDAL-Tower to request approach clearance. The pilot receives clearance through either the default waypoint APEST, or otherwise the slightly shorter path via MDEST or alternatively MARSH. In case of MARSH, ATC vectors the aircraft back to final while merging them behind arriving legacy traffic. Depending on the approach clearance, the second reporting point is either APEST or MDEST where the position is reported to KDAL-Tower and request filed to cross the runway for vertipad DF61. However, pilots may be told to 'hold short' of the runway crossing to allow for legacy arrivals on the runway. It is at the pilot's discretion how they decide to hold short, as long as they don't cross the runway.

B. Three Dissimilar Aircraft Models

Electric Vertical Takeoff and Landing (eVTOL) vehicles that can take off and land vertically like a helicopter and cruise like an airplane have the potential of increasing operational capabilities while maintaining a high degree of efficiency. These eVTOL vehicles exist in various configurations, such as multirotors, Lift-Plus-Cruise (LPC), and Tiltwing designs, among many others. This simulator study focuses on the three aforementioned designs. Each is optimized for dedicated mission profiles and behaves fundamentally different. More details of each concept vehicle as developed by the NASA Revolutionary Vertical Lift Technologies (RVLT) project, are given in Fig. 4 and can be found in [10, 11].

C. Autoflight Automation Concepts

The baseline aircraft equipage is centered around mid-term operations beyond Entry Into Service (EIS), in Good Visual Environment (GVE) conditions, with more than 6 to 10 operations per hour. This requires a higher navigation precision to enable segregated operations.

The baseline operational procedure requirements are based on Required Navigational Performance - Authorization Required (RNP-AR) approaches as baseline for precision and for the capability for curved approaches. RNP-AR is an advanced, high-precision instrument approach procedure that requires specialized aircraft equipage, pilot training, and specific operator authorization. It enables safer, more direct, and efficient approaches in challenging, mountainous, or congested environments due to narrower obstacle clearance areas. RNP-AR currently requires the following:

- No single pilot operations
- Specially trained crew
- Specially equipped and current aircraft equipage:
  - Navigation sensors to meet RNP-AR eligibility
  - Flight Director, Autopilot or HUD
  - Altimetry
  - Eligibility to perform Radius-to-Fix (RF) turns
  - Navigation database per AC20-138 and AC90-101A
  - Navigation map display suitable to control Flight Technical Error
  - Procedures for monitoring vertical deviation within 75 feet
  - Take Off and Go Around (TOGA) mode capability and Go-Around guidance
  - Operational pilot procedures to show compliance with AC90-101
  - Operational procedures for executing a missed approach prior to Decision Altitude (DA) (14cfr91.175, 91.176, 121.651, 135.225)

The aforementioned RNP-AR requirements are current transport capabilities, but it is not anticipated that entry to

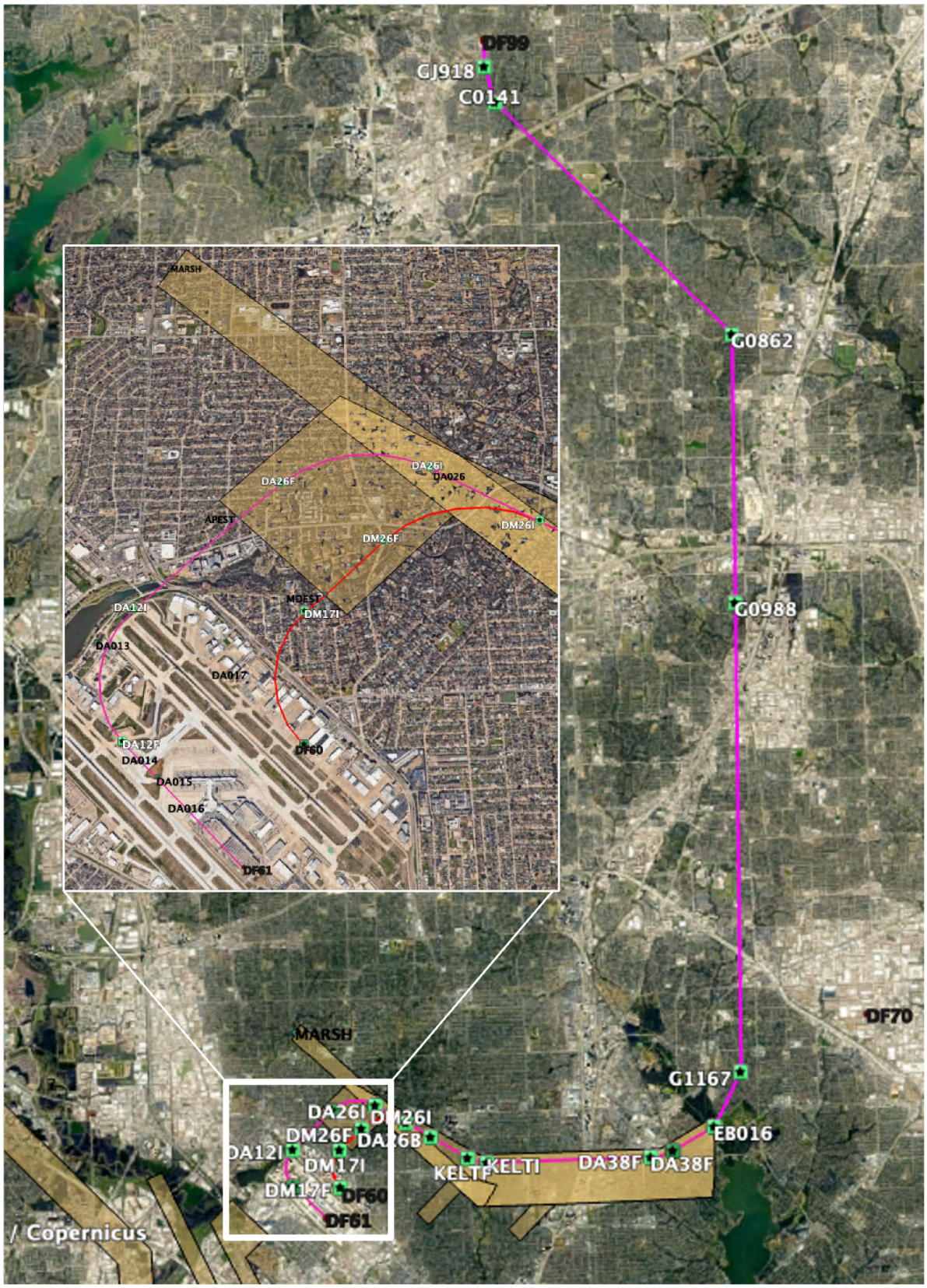


Fig. 2 Flight path and corridors from DF99 Frisco to DAL

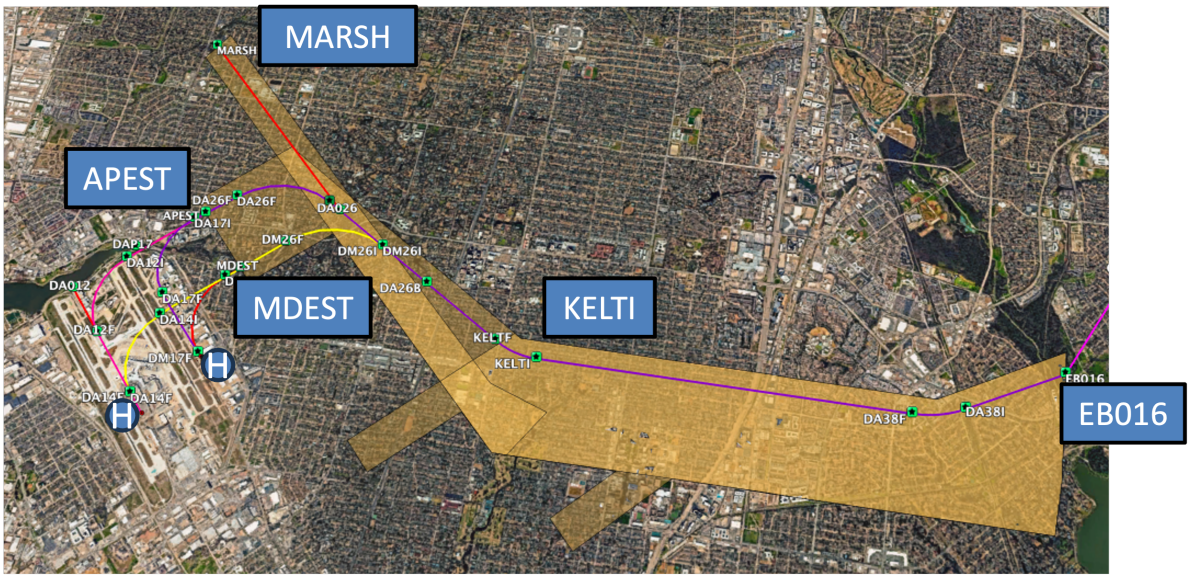


Fig. 3 AEP-3 explores AIS East KDAL Terminal corridor operations and approach procedures

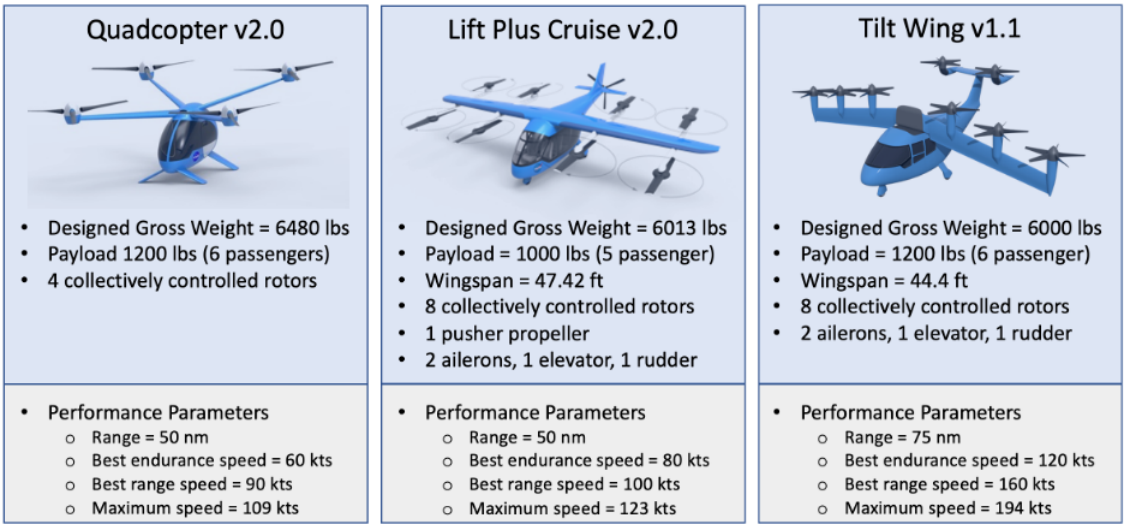


Fig. 4 NASA RVLT conceptual vehicle models, [10, 11]

service eVTOLs will have these capabilities. However, they are representative of the type of technology that might be needed to scale. As a last observation, 4D operations will require aircraft performance models, which most entrants' avionics do not support.

Figure 5 shows an RNAV chart that can be used if the vehicle relies on GPS position information with corresponding precision. This specific chart is for the aforementioned Dallas Love Field (DAL) Vertipad DF61 and is custom created for this experiment. Note that the DF61 vertipad is referred to as H61 which is the standard for helipads.

Operations are the driver for the equipage assumptions. In order to achieve the throughput and pace of operations desired for UAM and to navigate a dense complex airspace, a higher level of aircraft autoflight capabilities was assumed. Given the required precision of the corridor operations (0.1 RNP), this motivates the use of an RNP-AR approach as a baseline for the automation assumptions. Presently, this requires a navigational database and the use of Flight Director or Autopilot (FAA Advisory Circular AC 90-101A, [12]), necessitating autoflight capabilities.

Pilots have three levels of controlling the flight of the aircraft: 1) manually fly the aircraft (human within the loop) through the inceptors, commanding a simplified vehicle concept 2) a touchscreen Mode Control Panel interface for the autopilot system (human on the loop) and 3) a graphical Control Display Unit (CDU) human over the loop interface for the flight management system for flight planning and integrated autopilot modes (LNAV, VNAV). The automation architecture as used in this experiment is illustrated in Fig. 6.

Human within the loop

The manual inceptors connect directly to the flight controls, which encompass not only the simplified vehicle controls, but also envelope protection, 'outer loop' controls as well as 'inner loop' stability and control, which were all discussed in depth in [8].

The simplified vehicle controls are an industry representative Unified-like system in a 3+1 passive inceptor configuration, as shown in Fig. 7. The 3+1 passive inceptor configuration indicates that the right stick has three degrees of freedom (forwards-backwards, sideways and pivot) and the left stick has only one degree of freedom (forwards-backwards). Fig. 7 shows the commanded variables in the three different flight regimes, namely hover (with or without hover mode engaged), transition and forward flight. These flight regimes are distinguished based on the ground speed, and respectively defined by the ranges 0 to 20 kts groundspeed (only with hover mode engaged), up to 34 kts groundspeed and beyond. There is some offset from these values between accelerating and decelerating flight, to incorporate some hysteresis which avoids continuous back and forth mode switching near the threshold speed values. This figure also shows that the left stick controls speed, while the right stick commands vertical, lateral and directional movements. The commanded variables are shown for each control axis and flight regime. These simplified vehicle control concepts were developed previously and discussed in previous literature [7, 8].

Human on the loop

The pilot interface in this middle level is the Mode Control Panel (MCP), which interacts with the autopilot driving the guidance control laws. These guidance laws interface with the flight controls as well as the flight director. The MCP is integrated in a mid-term research Multi-Function Display (MFD) instead of a conventional panel with physical buttons, knobs and small numerical displays. This interface is modeled after the Garmin G3X and is shown in the right half of Fig. 12(a). A touchscreen is necessary to accommodate the limitations of the simulation facility. The autopilot includes transport-class autopilot modes, which are mapped throughout the full flight regimes. The autopilot can also drive a dual-cue flight director to provide guidance in manual flight which is compatible with the Unified-like controls. [13–15] provide more background on the Unified control concept.

Human over the loop

The pilot interface in this upper level is the mid-term research Control Display Unit (CDU) and Flight Management System (FMS), which are operated via a touchscreen interface as shown in the right half of Fig. 12(b), and interact with the previously discussed autopilot. The FMS contains a navigation database (ARINC424) that is consistent with an industry representative FMS. The flight planning and 4DT features are also representative of current transport capabilities, such as Estimated Time of Arrival (ETA) and Required Time of Arrival (RTA), which are discussed next. The aircraft were required to arrive at certain points of interest at a specific time to control aircraft spacing. The pilots were given two choices of how to accomplish meeting the time constraints: monitoring the Estimated Time of Arrival (ETA) on the CDU pages or using a Required Time of Arrival (RTA) function in Flight Management Computer (FMC) which would provide departure time and speed guidance [16]. The FMC RTA function operates in two distinct modes: ground mode and flight mode. In ground mode, the FMC computes the ETA (Estimated Time of Arrival) at the required

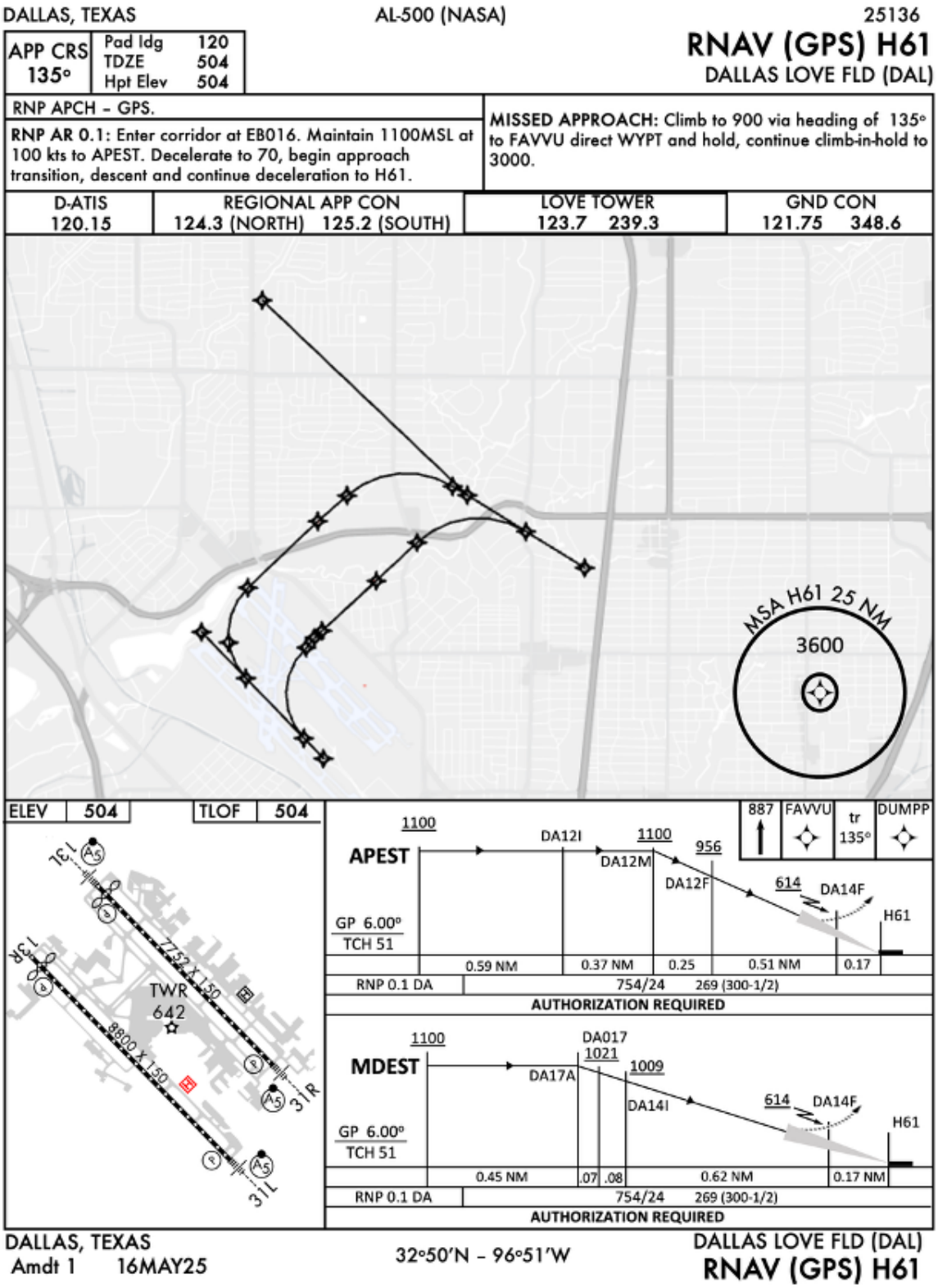


Fig. 5 RNAV chart for DAL to vertipad DF61

waypoint based on the speed profile previously entered into the FMC. It then calculates the recommended take-off time to meet the time constraint at that speed. The recommended take off time is displayed on the FMC RTA page in the following format: HH:MM:SS. Once that time has been reached, take-off time display changes to "NOW". Once the aircraft takes off, the FMC continuously monitors ETA at the RTA waypoint. If the difference exceeds the predefined required tolerance (set at +/- 12 seconds), the FMC recalculates aircraft speed to satisfy the time constraint. If the aircraft is late beyond the required tolerance when flying at maximum speed, or early while flying at minimum speed, the FMC notifies the pilot via scratchpad message: "UNABLE RTA". Operation in air mode is very similar with the main exception that recommended take-off time is not present. When a time constraint is entered, the FMC immediately re-calculates aircraft speed to meet that time constraint. The remainder of RTA functionality is as described for ground mode.

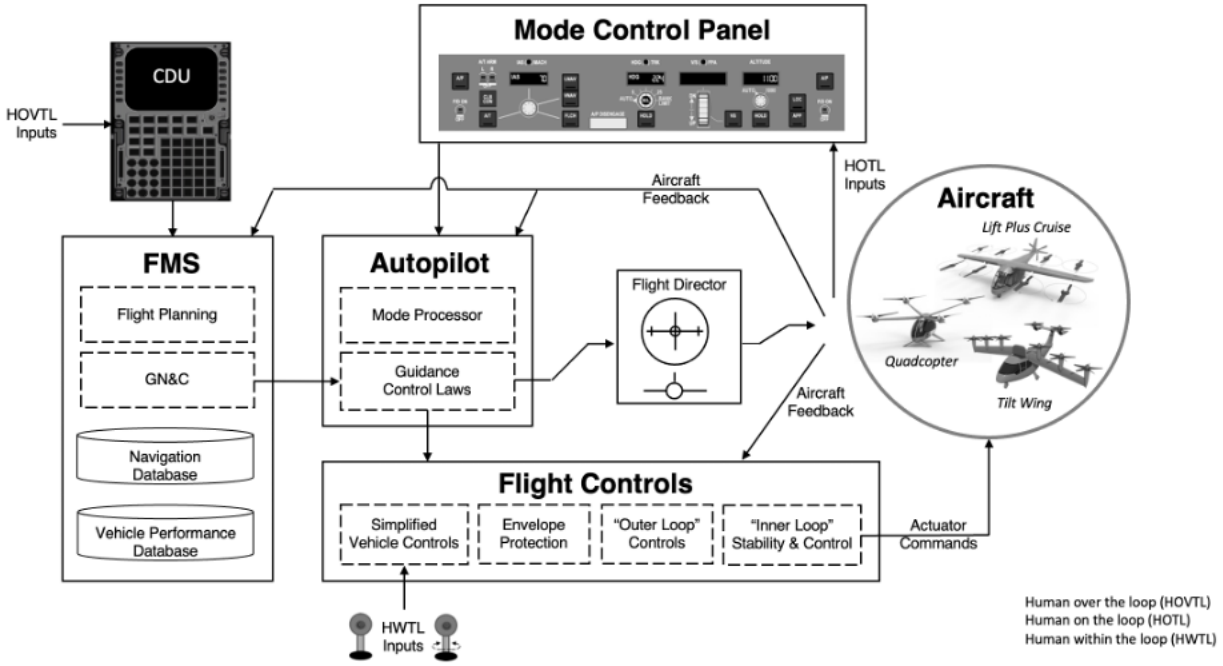


Fig. 6 Automation architecture

Flight Regime	Left Stick	Right Stick			Groundspeed
	Speed (Accelerate / Decelerate)	Vertical (Descend / Climb)	Lateral (Go Left / Go Right)	Directional (Yaw Left / Yaw Right)	
Hover (Hover Engaged)	Longitudinal Velocity Cmd	Vertical Speed Cmd	Lateral Velocity Cmd	Heading Rate Cmd	(0-20 KGS)
Transitional	Acceleration Cmd*	Vertical Accel Cmd FPA Hold	Bank Cmd		(0-34 KGS)
Forward Flight		FPA Rate Cmd[1]	Roll Rate Cmd	Sideslip Cmd	(34+ KGS)

*Hover arm/engage results in nominal 2 kt/sec decel
(1) FPA Rate Cmd FPA Hold (for Quad)

Fig. 7 Simplified Vehicle Control concept: Unified-like Command Concept with semi-automated Assistive Hover Automation (AHA)

III. Study Description

This section discusses the facility used for the experiment in Sec. III.A, together with a discussion of the scenarios and their evaluation metrics in Sec. III.B and a brief description of the participants in Sec. III.C.

A. Vertical Motion Simulator

The Vertical Motion Simulator (VMS) is the ideal facility to evaluate lift mode transitions and low speed operations because of its large motion envelope. The VMS motion system, shown in Fig. 8 and Fig. 9, is an uncoupled six-degree-of-freedom research motion simulator, with different interchangeable cockpit cabs and configurable flight deck instrumentation systems, wide-view outside visual display systems, electric control loaders and a high fidelity motion system. It is located in, and partially supported by, a specially constructed 120 ft tower. More information about the simulator can be found in Ref. [17–19].

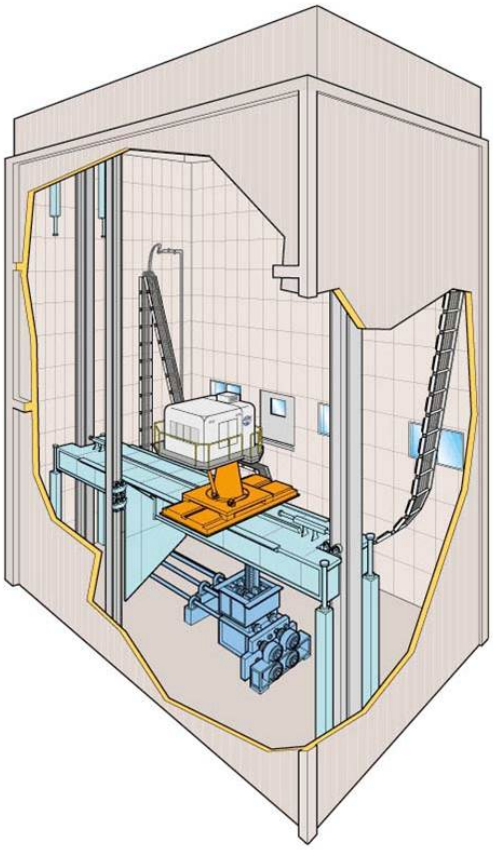


Fig. 8 Drawing with layout of the Vertical Motion Simulator

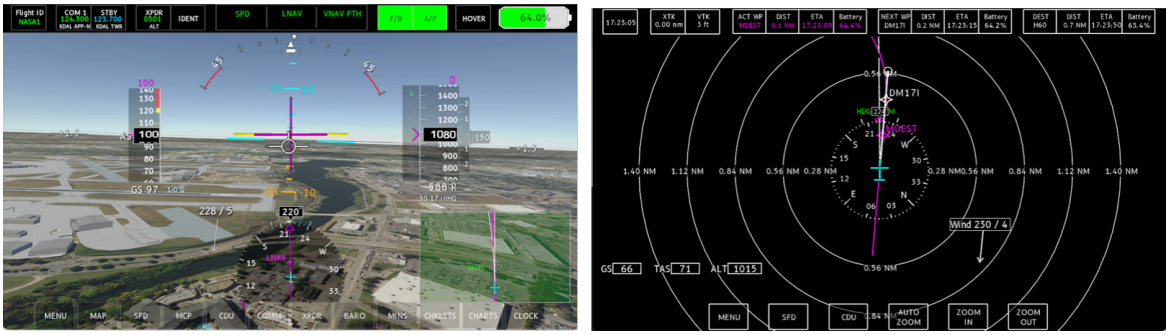


Fig. 9 Picture of the VMS cab on the beam

For this study, the cockpit shown in Fig. 10, was configured for a single pilot in the front seat and a flight test engineer in the back seat. The installed inceptors consisted of left and right passive sidesticks. The left sidestick serves as accelerator/decelerator, the right stick has three degrees of freedom for vertical, lateral and directional by twist. The pedals serve only as brakes. The out-the-window (OTW) visual system provides a 130 degree field-of-view, as well as left and right chin windows. Two liquid crystal display (LCD) touchscreens were used to display flight instrumentation. These Multi-Function Displays (MFD) were representative of a Primary Flight Display (PFD) (Fig. 11(a)) and a Navigation Display (ND) (Fig. 11(b)). Both are equipped with touch buttons to toggle between full screen or split screen modes. The split screens show the Mode Control Panel (MCP) next to the PFD (Fig. 12(a)) and the Control Display Unit (CDU) next to the ND (Fig. 12(b)). Additionally, local traffic is depicted on the ND as seen in (Fig. 13). Other combinations are possible as well.

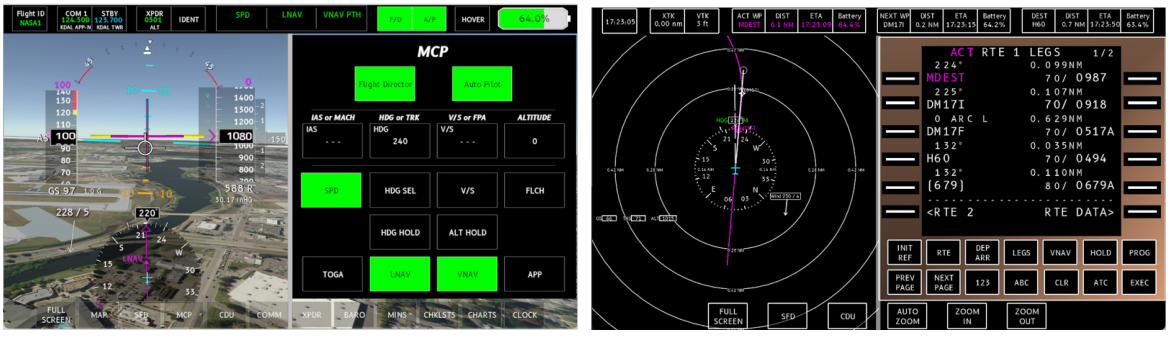


Fig. 10 VMS Cockpit



(a) Primary Flight Display (b) map display

Fig. 11 Cockpit displays used during the simulator experiments, full screen mode



(a) Primary Flight Display with Mode Control Panel (b) map display with Control Display Unit

Fig. 12 Cockpit displays used during the simulator experiments, split screen mode

B. Test Matrix and Scenarios

Experiment data were collected across three similar scenario sessions, each session involved one of the three aforementioned vehicles Lift-Plus-Cruise, Quadcopter and Tiltwing. The order of the three scenario sessions was randomized over all pilots, to minimize learning effects across vehicle models. Each session includes 3 blocks with varying procedures, automation, winds and traffic conditions summarized below:

1) Departure and Enroute (Frisco to corridor entry): 1 run
   - Automation:
     - Pilot chooses either ETA or RTA
     - Flight Director, optional autopilot after manual takeoff
   - Winds: Light 5 kts (4 kts steady + 1 kt gusts) enroute headwind vs enroute tailwind
2) Corridor Operations: 5 runs
   - Automation: Flight Director or autopilot
   - Route variations:
     - APEST to DF61: with and without hold short (2 runs)
     - MDEST to DF61: with and without hold short (2 runs)
     - MARSH to DF61: with vectors to DF61 (1 run)
   - Winds: Variable 5 kts (4 kts steady + 1 kt gusts)
3) Approach and Landing: 4 runs
   - Automation: Flight Director
   - Route variations:
     - APEST to DF61: nominal and alternate pad (2 runs)
     - MDEST to DF60: nominal and alternate pad (2 runs)
   - Winds: Moderate 10 kts crosswind (8 kts steady + 2 kt gusts)

Each scenario also had traffic which was designed for out-the-window (OTW) operations, ATC communication and maintaining minimum separation. The traffic activity consisted in total of 8 aircraft that appeared at various times throughout the run, namely two Boeing 737 airliner arrivals to KDAL runways 13L and 13R, two Boeing 737 airliner departures from KDAL runways 13L and 13R, two General Aviation (GA) aircraft in Class G and E airspace, one UAM departure from KDAL DF61 vertipad and one UAM arrival to KDAL DF60 vertipad. For example, the hold short ahead of the runway crossing in the corridor operations was due to a 737 arrival on that runway. Other select conflict scenarios were crossing GA aircraft in class E airspace and a slow preceding quad in the corridor. Pilots could detect all traffic out-the-window at realistic distances, but also by means of the usual state-of-the-art symbology on the Navigation Display, as shown in Fig. 13. Fig. 14 shows the orientation of the nominal and alternate vertipads at DF61, with the nominal pad on the right hand side and the alternate on the left. The alternate pad was only relevant in the approach and landing scenario. Note the vicinity of the parked vehicles close to the vertipad.

Each scenario block will be further described in detail next.



Fig. 13 Navigation Display with traffic info

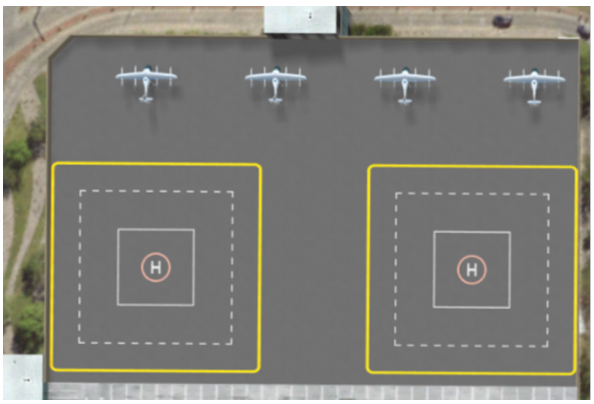


Fig. 14 Nominal and alternate vertipads at DF61

1. Block 1: Departure and Enroute (Class G & E)

This block consists of only one run, along the flight plan segment taking off at Frisco and flying to the corridor entrance depicted in Fig. 15. This involves a departure, enroute and arrival transition from DF99 to EB016. The Scheduled Departure Time is 17:10:00Z (Zulu time) (which is 12:10:00 CDT (Central Daylight Time)) and the Scheduled Arrival Time (STA) at waypoint EB016 depends on the vehicle, namely 17:20:21Z for the LPC, 17:20:41Z for the quadcopter which is the slowest of the three and 17:17:14Z for the tiltwing which is the fastest of the three. Independent variables are:

- Automation: Estimated Time of Arrival (ETA) or Required Time of Arrival (RTA), at the pilot's discretion
- Wind: headwind vs tailwind (4 kts steady component, gusting up to 5 kts)
- Traffic: nominal and conflicting scenarios (GA aircraft crossing the path)

The mission metrics are first of all 4DT compliance metrics, namely vertical track error, lateral/crosstrack track error, and temporal track error. The other metrics are the STA error at corridor entrance (EB016), minimum vehicle separation, communication/clearance timing and strategy, and workload, as described in Table 1.

Table 1 Trajectory metrics specifications for departure and enroute scenario

Maneuver	Desired	Adequate
vertical track error	± 125 ft	± 250 ft
lateral/crosstrack error	± 750 ft	± 1500 ft
temporal track error	± 30 s	± 60 s
STA error @ EB016	± 30 s	± 60 s

2. Block 2: Corridor Operations (Class B)

This block consists of five runs, along the flight plan segment from corridor entrance to landing. This includes an arrival, approach transition, approach and landing from EB016 to DF61. Independent variables are:

- ATC clearance options:
  - "Proceed via Approach East to vertipad DF61, report APEST"
    - "Hold east of runway 13L"
    - "Proceed across of runway 13L"
  - "Proceed via Mideast to vertipad DF61, report MDEST"
    - "Hold east of runway 13L"
    - "Proceed across of runway 13L"
  - "Proceed via MARSH to vertipad DF61, expect vectors"
- Winds: variable (4 kts steady component, gusting up to 5 kts)
- Traffic:
  - Nominal
  - Slow quad ahead in corridor, on MDEST approach to DF60
  - Hold short for landing traffic on runway 13L (only via APEST and MDEST)

The three potential approach transitions are shown in Fig. 16. The mission metrics are clearance compliance, lateral and vertical track compliance metrics, vehicle spacing within corridor and workload, as described in Table 2.

Table 2 Trajectory metrics specifications for corridor scenario

Maneuver	Target	Desired	Adequate
vertical track error	–	± 125 ft	± 250 ft
lateral/crosstrack error	–	± 750 ft	± 1500 ft
speed range (up to DA12I or DA14I)	70 – 100 kts	65 – 105 kts	60 – 110 kts
speed range (after DA12I or DA14I)	70 kts	65 – 75 kts	60 – 80 kts

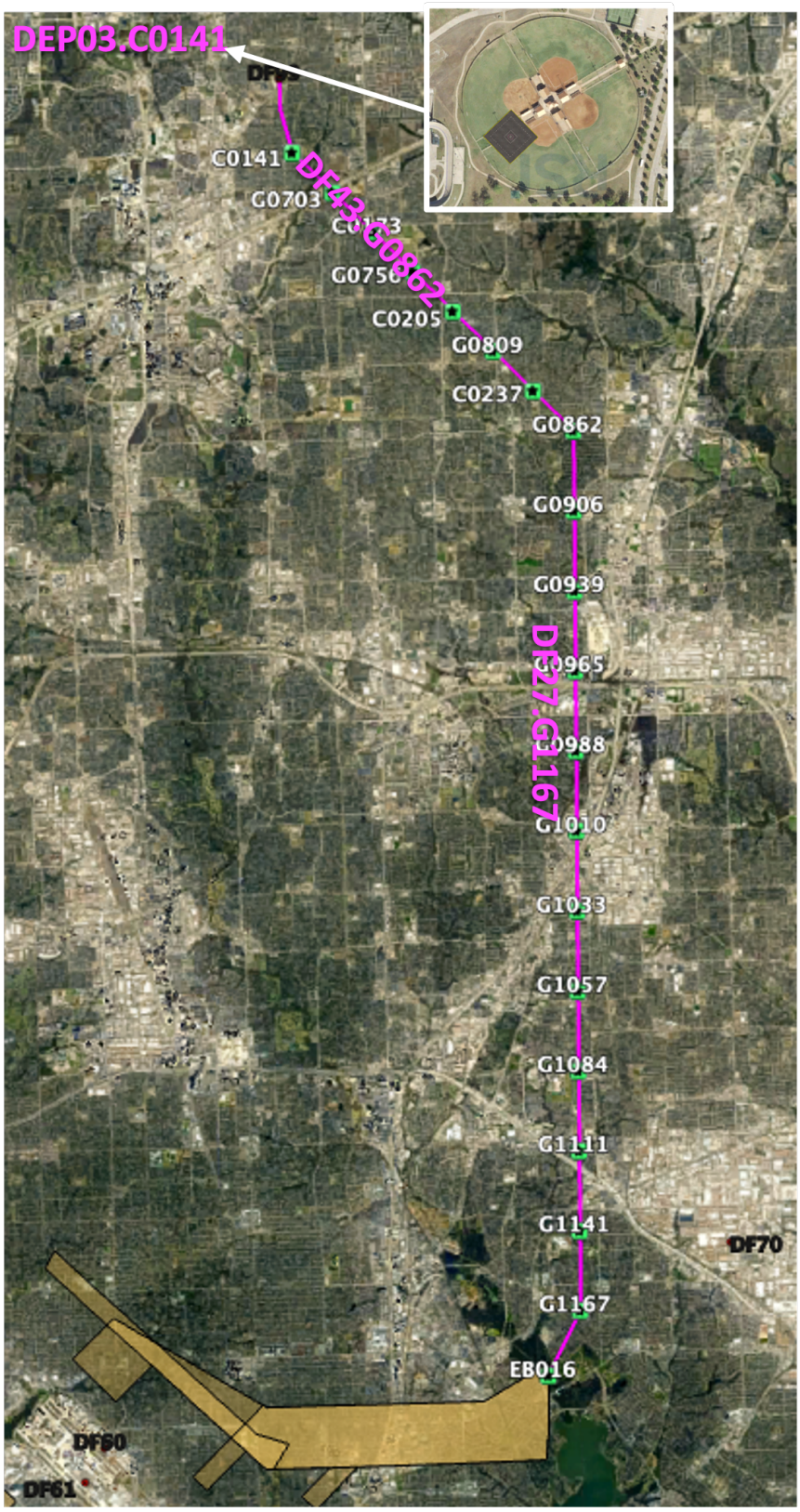


Fig. 15 Block 1: departure and enroute



Fig. 16 Block 2 consisting of 3 approach transitions in corridor

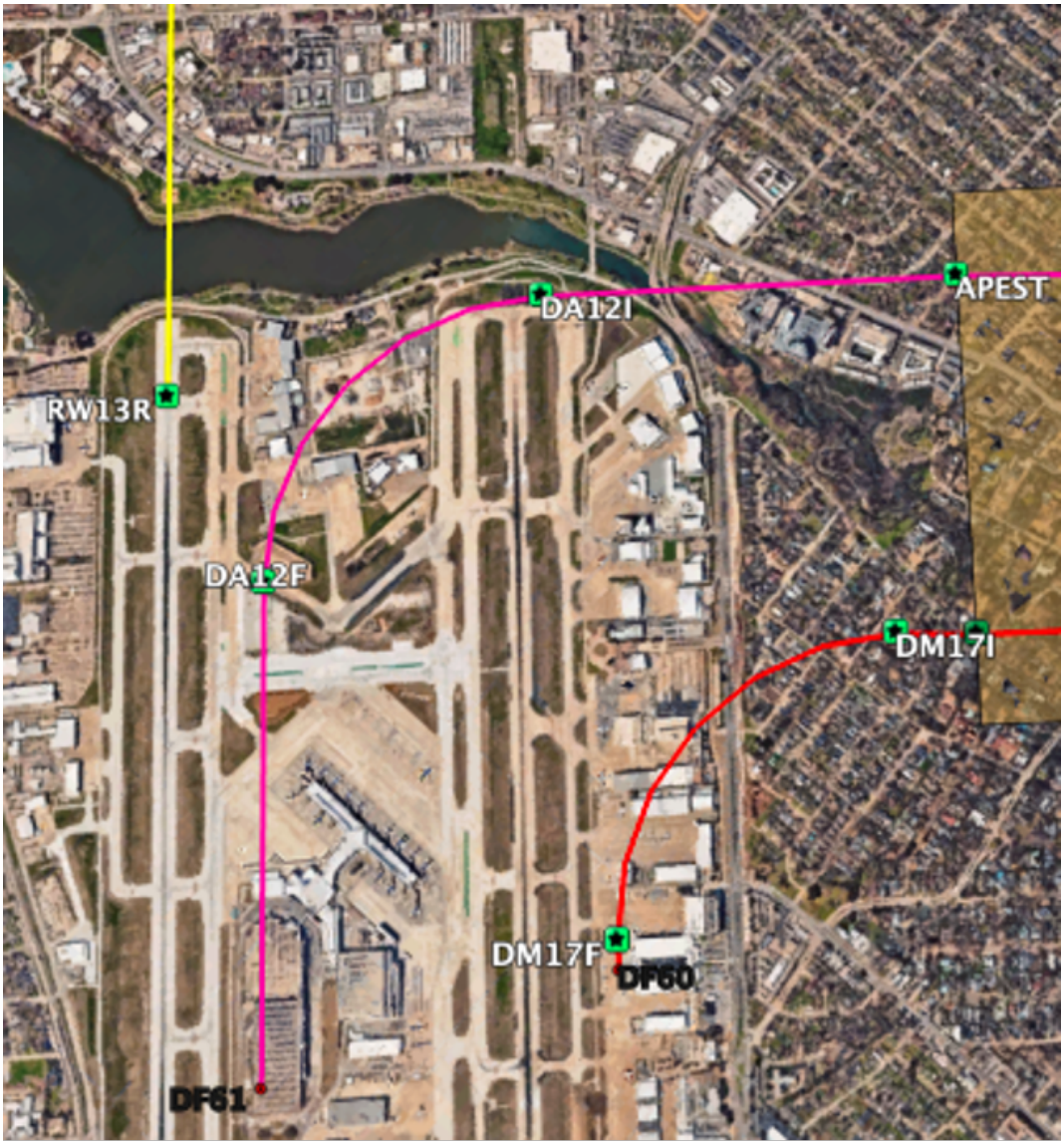


Fig. 17 Block 3 consisting of straight and curved approaches to landing

3. Block 3: Approach & Landing (Class B)

This block consists of four runs, along the flight plan segment approach transition to landing (Fig. 17). Independent variables are:

- Approach: straight (from APEST via Z14 to DF61) vs curved (from MDEST via Z13 to DF60)
- Automation: manual
- Wind: 10 kts left/right crosswinds (8 kts steady component, gusting up to 10 kts)
- Traffic: none
- Alternate pad option (randomized):
  - 2 nominal runs (1 for each vertipad DF60 and DF61)
  - 2 alternate runs (1 for each alternate vertipad DF60 and DF61)

In the alternate pad option, ATC calls out the alternate pad about 0.3 nm from the vertipad. DF60 has an alternate pad just beyond the main pad and the alternate pad of DF61 is to the left of the main pad seen in Fig. 14. The locations of both DF60 and DF61 are depicted in Fig. 18.

Mission metrics are lateral and vertical track compliance metrics, landing metrics, touchdown performance and workload, as described in Table 3.

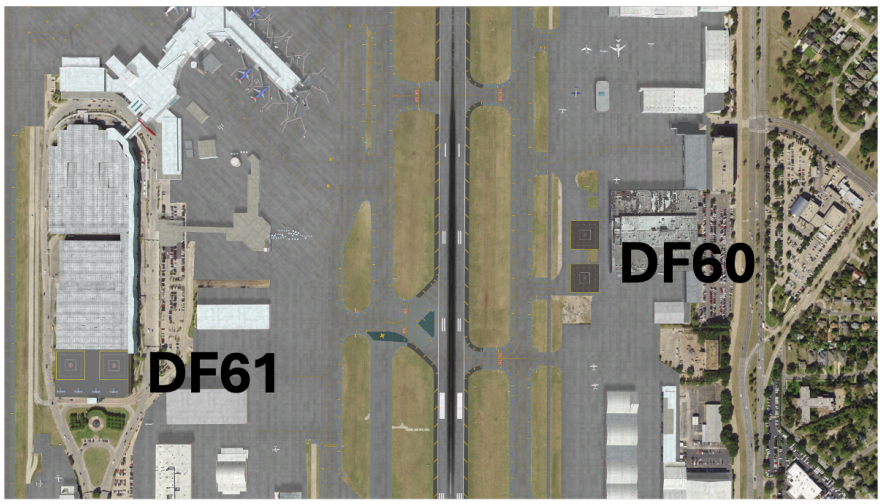


Fig. 18 Location of the vertipads at DF60 and DF61

Table 3 Trajectory metrics specifications for landing scenario

Maneuver	Desired	Adequate
vertical track error	± 125 ft	± 250 ft
speed error	± 5 kts	± 10 kts
touchdown distance to touchdown target	± 5 ft	± 10 ft
vertical speed at touchdown	≤ 240 ft/min	≤ 360 ft/min
longitudinal speed at touchdown	-0.5 / +2 kts	-1 / +4 kts
lateral speed at touchdown	± 1 kts	± 2 kts

C. Participants and Procedure

Due to the very specific nature of this experiment with emphasis on future operations, there was no qualified pilot pool for the participants. Participants had very diverse pilot backgrounds. There were 9 pilot participants across industry aircraft OEM, avionics OEM, FAA Flight Standards organization (responsible for approving UAM operations) and NASA flight test pilots.

The program was split up over two consecutive days, where the first day focused on training. The Aircraft Flight Manual (AFM) was distributed prior to travel to Ames, followed by one day in the ACEL-RATE simulator (see Fig. 19) where training focused on procedures, aircraft performance, automation, inceptor strategy, UAM environment and operations, eye tracking and subjective measures. The training day was completed by means of a post-training questionnaire.

The second day was a data collection day that started with familiarization with the Vertical Motion Simulator (VMS) seen in Fig. 20, since this was the first time that most participants worked with this research facility. Thereafter followed the scenario data collection runs, which focused on flight technical performance via the logdata, subjective ratings of the pilots via the NASA Taskload Index (TLX) [20], and also eye tracking. The data collection day was completed by means of a post-sim questionnaire and debrief.

IV. Results

The results, which include flight performance metrics, airspace communication compliance, and subjective feedback, are presented in the same sequence as the scenario blocks, discussed earlier in Sec. III.B, followed by more focused sections on battery usage and workload ratings.

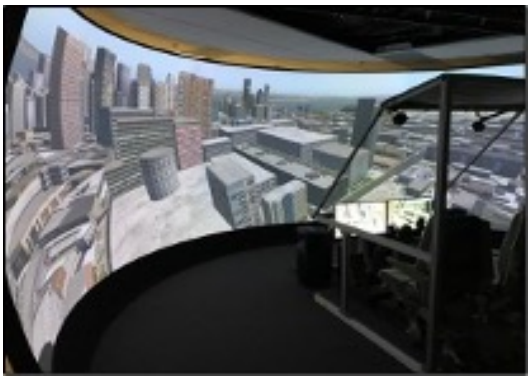


Fig. 19 ACEL-RATE lab used for training

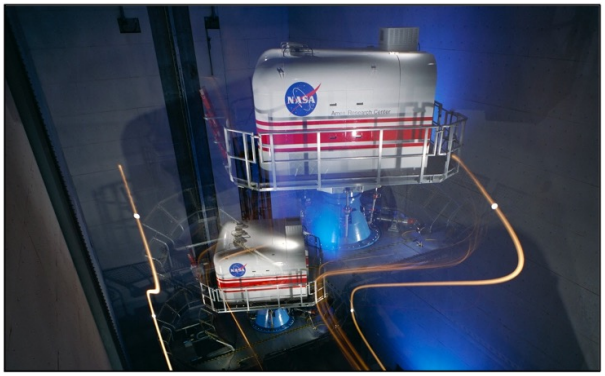


Fig. 20 Vertical Motion Simulator for data collection

A. Block 1: Departure and Enroute

The observations discussed here refer to the scenario block as described in Sec. III.B.1. Across all runs, pilots took off early, before their scheduled departure time. The timing metrics for departure are shown in Fig. 21. On average pilots took off about 30s early from Frisco, but the most frequent occurrences were about 50s (8 runs out of 25) and 10s early (5 runs out of 25). All pilots chose to use RTA automation to meet the STA at waypoint EB016 near the corridor entrance, instead of monitoring the ETAs themselves along the waypoints in the FMS. For nominal runs without traffic conflicts, all pilots crossed EB016 in the desired range which was within +/- 30 seconds of the pre-specified STA, as shown in Fig. 22. This figure shows the difference in STA at EB016 for the three different vehicles, reflecting the earlier arrival time for the faster tiltwing and the later arrival time for the slower quadcopter. The reference times for each vehicle in Fig. 22 match with the corresponding vehicle dependent STA values as specified in Sec. III.B.1. One run deviated from the overall trend, but this was because of a perceived traffic conflict and therefore this one pilot did not make the STA within desired or adequate tolerances.

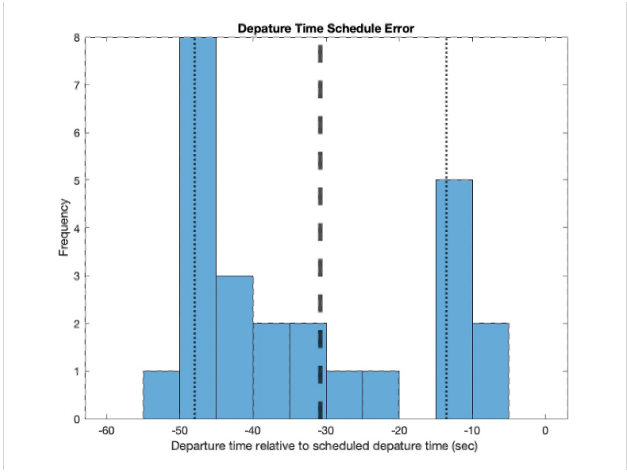


Fig. 21 Departure time schedule error

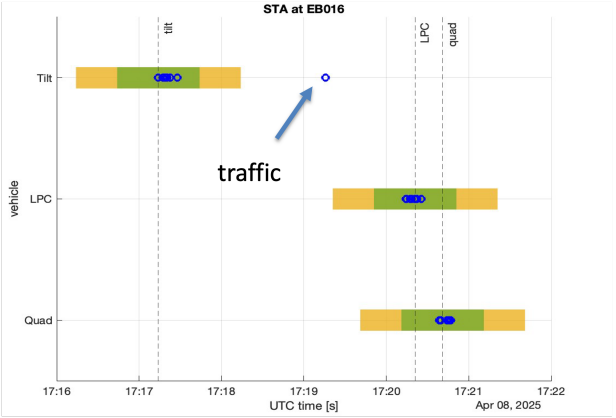


Fig. 22 Scheduled time of arrival at EB016

A large spread was observed in the timing when pilots requested to enter the class B corridor, however most tended to be early. Some pilots mentioned that they would have preferred this clearance pre-departure, but ATC might not be capable to do so, depending on their workload and ability to predict ahead in time for this duration of flight.

Figure 23 shows the deviations in time to track (TTK) with respect to the distance along the flightpath towards the touchdown (TD) point. The takeoff location is 26 nm away from the arrival point along track. The figure shows that all pilots took off early, but there was a large spread in hover time above the vertipad, before they started their journey along the flightpath. Fig. 23 shows subplots for the different vehicles (from top to bottom LPC, quadcopter and tiltwing) with vertical dashed lines indicating the waypoints (WP) and trajectory change (TC) points. Note that the different

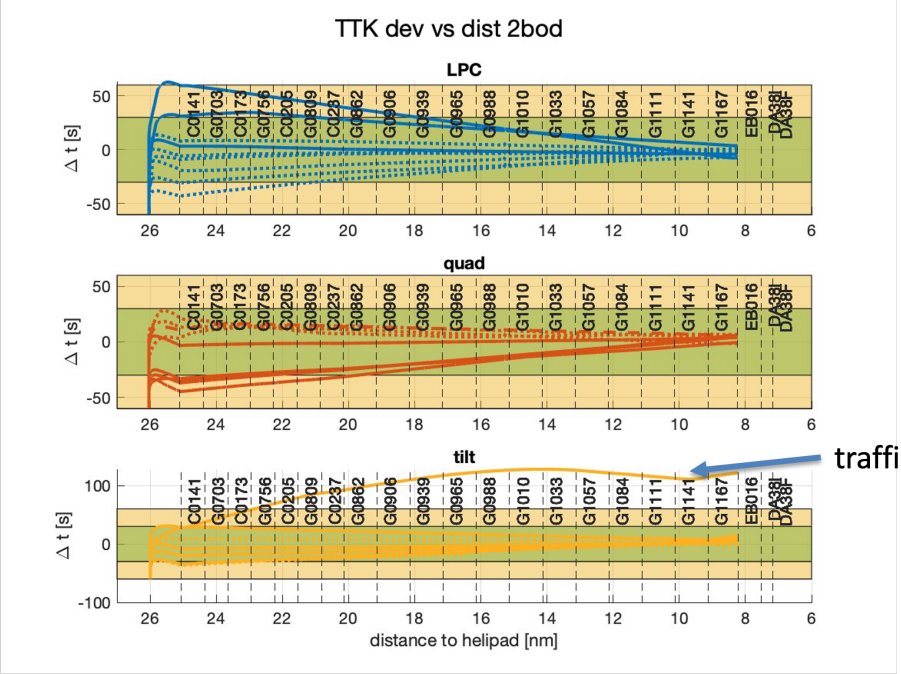


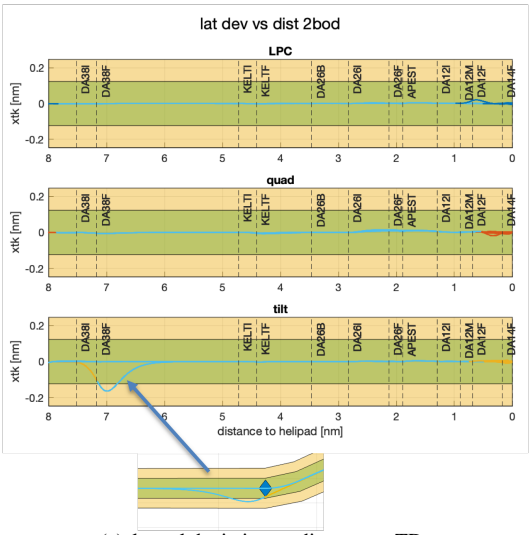
Fig. 23 Time to track deviations vs distance to TD

performance levels of each aircraft design result in slightly different climb and descent profiles and thus variations in the distances between WP and TC points. The graphs also distinguish between headwind (dotted lines) and tailwind (solid lines). The graphs show a symmetrical spread in TTK deviation at the end of the hover phase after takeoff for the LPC and tiltwing, wider for the LPC (still mostly adequate) than for the tiltwing (mostly desired). The TTK deviation at the end of hover skews towards early for the quadcopter, but still in the adequate range. Fig. 23 also shows how the RTA automation uses the full length of the track to gradually eliminate the TTK error and ends up within desired bounds at EB016, except for the tiltwing run that was affected by perceived traffic conflicts.

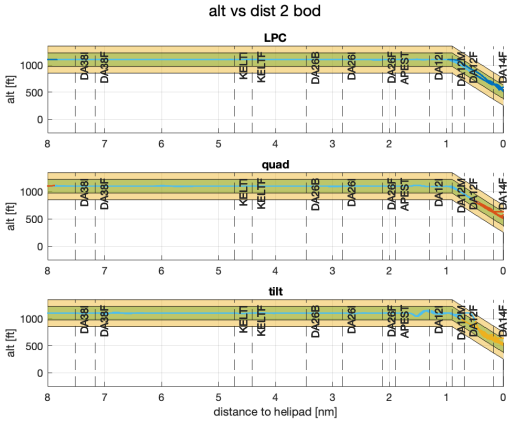
B. Block 2: Corridor

Figure 24 shows the lateral, altitude and speed deviations with respect to the relevant performance metrics in the corridor scenarios for the nominal APEST runs without conflicting traffic. Each subfigure shows graphs per vehicle design: top to bottom show results for LPC (in dark blue if flown manually), quadcopter (in red if flown manually) and tiltwing (in amber if flown manually). The cyan color for any vehicle design indicates that the autopilot was active at that time. The lateral deviations in Fig. 24(a) show that most runs stayed well within the desired RNP precision of 0.1 nm. One run of the tiltwing only achieved adequate but not desired performance. Closer inspection shows that this happens at an initial turn early in the flight plan, when the pilot hadn't engaged the autopilot yet, as illustrated by the inset figure. The altitude deviations in Fig. 24(b) show overall desired performance. Fig. 24(c) shows the speed performance and the corresponding metrics, such as the mandatory slow down to 70 kts ahead of WP DA12I. Most pilots followed the speed restrictions within the desired range. One run of the LPC missed the deceleration phase due to FMS mode confusion. All runs slow down towards the end because they are approaching the helipad.

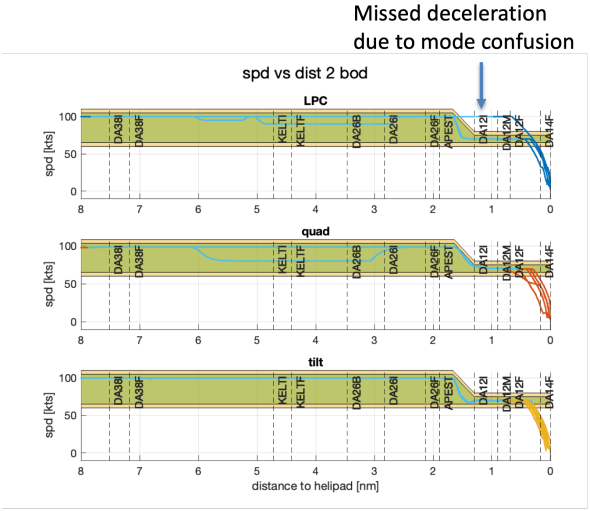
Figure 25 shows the lateral, altitude and speed deviations with respect to the relevant performance metrics in the corridor scenarios for the MDEST runs with a slower quadcopter ahead in the same corridor as conflicting traffic. This figure is presented in a similar way as Fig. 24. Some pilots tried manual evasive maneuvers laterally and/or vertically, but this was not always within the required tolerances, as can be observed in Fig. 25(a) and 25(b). Later training advised against executing these kinds of evasive maneuvers. Most pilots however slowed down for traffic ahead, either manually or via the autopilot, which can be distinguished in Fig. 25(c) based on the color coding. Two tiltwing runs (the faster tiltwing had the highest relative speed difference with the slower quad) ended up too slow, temporarily below the min corridor speed of 70 kts, even with tolerances. One slowed down manually, the other one with the autopilot, where the pilot exceeded the tolerances twice.



(a) lateral deviation vs distance to TD

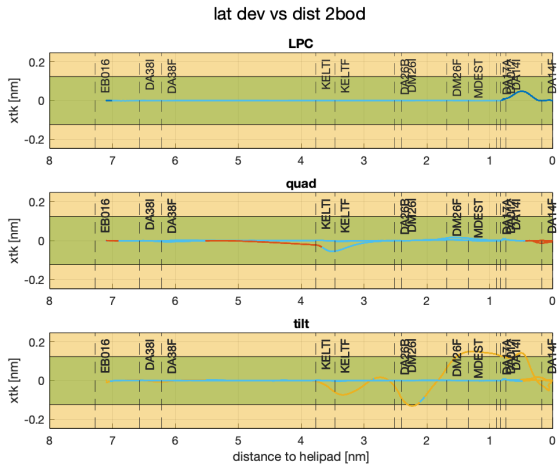


(b) altitude deviation vs distance to TD

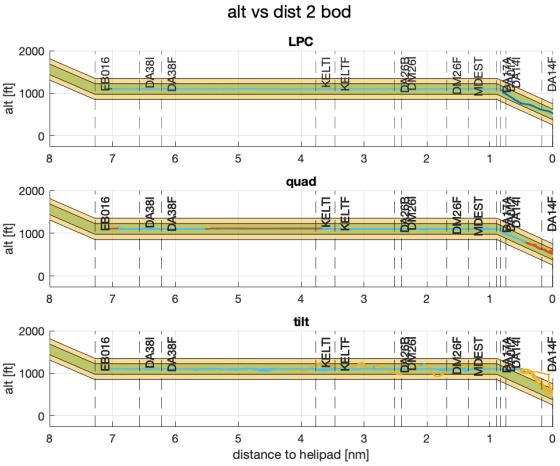


(c) speed deviation vs distance to TD

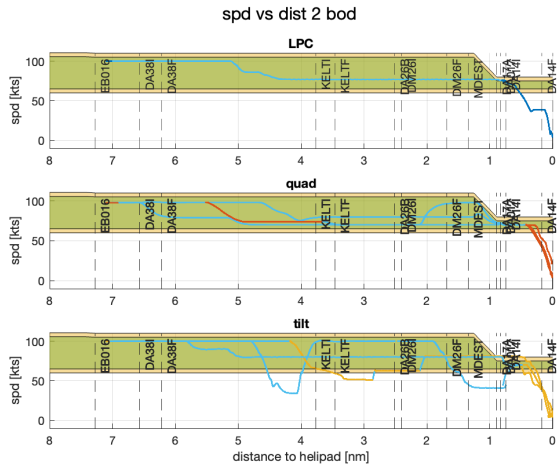
Fig. 24 Performance metrics in corridor for nominal APEST runs



(a) lateral deviation vs distance to TD



(b) altitude deviation vs distance to TD



(c) speed deviation vs distance to TD

Fig. 25 Performance metrics in corridor for MDEST runs with a slow quadcopter ahead

Overall, for both the departure and enroute scenario, it was clear that the expected RNP levels were well achievable with the automation available on board. However, when automation was not used, regardless of reason or intention, the ability to maintain the same RNP levels decreased. Multiple pilots commented on this difficulty stating: ”For the RTA and width of those corridors I think the autopilot is required especially for this vehicle spacing” and ”Definitely want autopilot, especially for single pilot.”

Pilots typically had to request clearance twice in the corridor runs: once at KELTI and once at either APEST or MDEST depending on the approach clearance. No clearance was required at MARSH; however, pilots expected vectors back to the final approach course. Typically, it was expected that they would request clearance when the relevant waypoint was active, i.e. between the previous waypoint and the relevant waypoint. Figure 26 shows the timing of these clearance requests with color coding to indicate the different timing groups. Dark green is on time, between the previous waypoint and the point of interest. Light green means early, prior to the previous waypoint. Amber represents a close call when they requested clearance at the actual waypoint of interest (within 300ft) and red shows that they were late, more than 300ft beyond the point of interest. The bar plots also distinguish between the different traffic scenarios, namely nominal, slow quad and hold short. A large spread over time was observed with the KELTI reporting due to the long preceding leg, but most pilots reported on time. For the KELTI runs, the pilot had to wait for ATC communication with other traffic to finish before reporting by themselves in more than ten runs. Overall, there were impacts of mode confusion, distraction and communication congestion.

Pilots were told to report at APEST and MDEST specifically, and most reported immediately when APEST or MDEST became their active waypoint. For the hold short, one ATC call was interrupted and there were five runs when the pilot waited for other communications to finish. The one late communication at APEST nominal happened because of mode confusion. One slow quadcopter traffic case on APEST transition resulted in a different timing because the vehicle went off track. In contrast with the other scenarios, no early reports were observed for the slow quad scenario when the pilot was cleared for the MDEST transition. This is likely due to the slow quad being on the same approach transition meaning the pilot spent a longer time occupied with maintaining safe separation. Moreover, for one run the slow quadcopter resulted in late reports at both KELTI and MDEST. For the hold short traffic cases, pilots were more likely to report early regardless of approach transition indicating that they may have spotted the upcoming conflict on their own. In the hold short, some reports were pre-empted by ATC because of traffic; there could have been more close calls if these reports were not pre-empted. Despite the busy traffic in these scenarios, one pilot “expected more traffic especially the legacy and eVTOL traffic”.

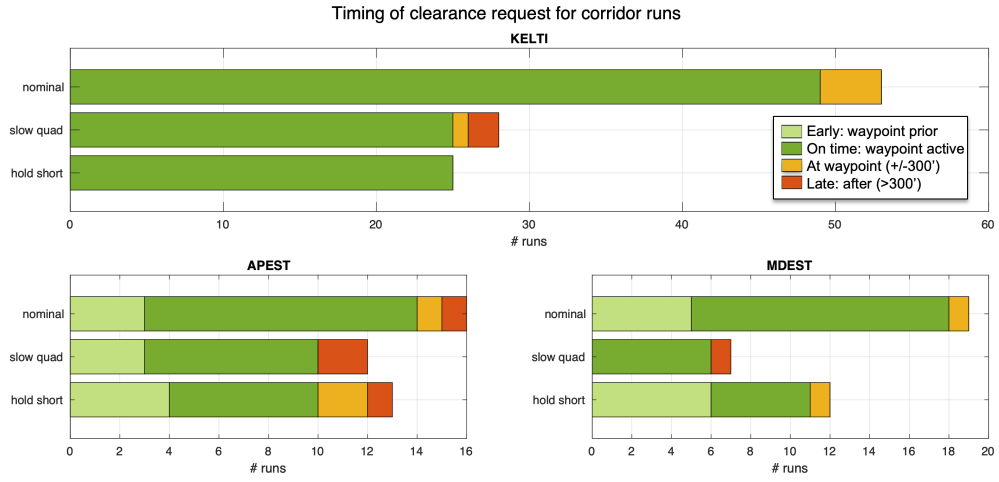


Fig. 26 Corridor communication compliance

Figures 27 – 30 show relevant information for the hold short traffic scenarios. The locations of the APEST and MDEST reporting points depicted in Figure 27, are only 0.59 nm from the runway. Given the speed constraints in the corridor (70 - 100 knots), the time to runway crossing is approximately 61 - 87 seconds. Pilot comments address this stating ”report half mile from the airport. . . always struck me as very tight.” The ground track for each aircraft design in the hold short scenarios is seen in Figure 28. Some interesting observations here are that seven out of nine pilots completed a manual left-hand turn, prioritizing separation from the legacy traffic that is approaching from the right.

However, one pilot out of nine executed a right hand turn, prioritizing to keep the approaching traffic in the field of view. One pilot preferred to slow to a hover which reduced the occupied airspace at the cost of battery usage. Fig. 29 shows the minimum distance from the runway crossing during the execution of the hold short maneuvers for all runs. All pilots avoided the runway crossing, but there is a large spread in the minimum distance, several of the pilots getting closer than 800 ft of the runway. The tight time window and manual execution in most runs resulted in significant vertical deviations. While most pilots remained in the adequate margins for altitude, one quadcopter run resulted in an extreme altitude excursion, as shown in Fig. 30(a). Slowing down to hover also led to more serious altitude excursions. The speed excursions in the turns were minimal, as illustrated in Fig. 30(b). MCP initiated heading turns stayed well inside the desired ranges overall.

It should be noted that these xTM procedures must account for a diversity of vehicle designs requiring sufficiently wide constraints to accommodate a wide range of performance characteristics. For example, an aggressive hold short maneuver in a quadcopter is achievable around 70 knots; however, it risks severe Pilot Induced Oscillations (PIOs) if flown near its maximum speed of 100 kts. The wide velocity window in the corridor (70 - 100 knots) allows for safe operating speeds across different vehicle designs, even when aggressive maneuvering may be required.

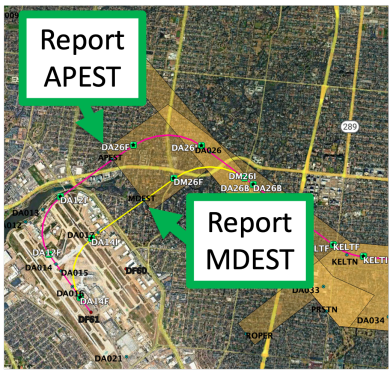


Fig. 27 Report locations for APEST and MDEST

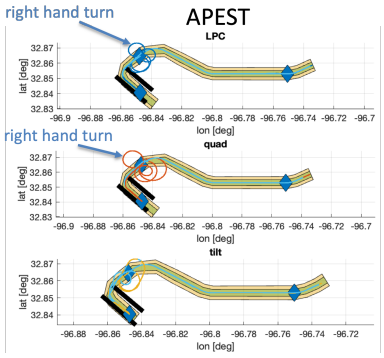


Fig. 28 Ground tracks for hold short scenarios on APEST approach transition

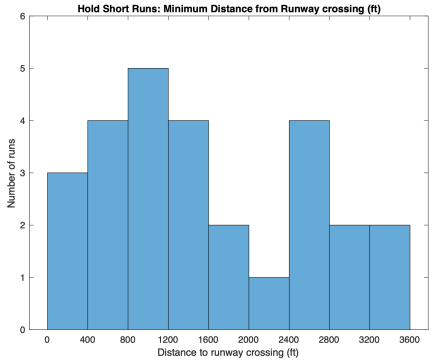
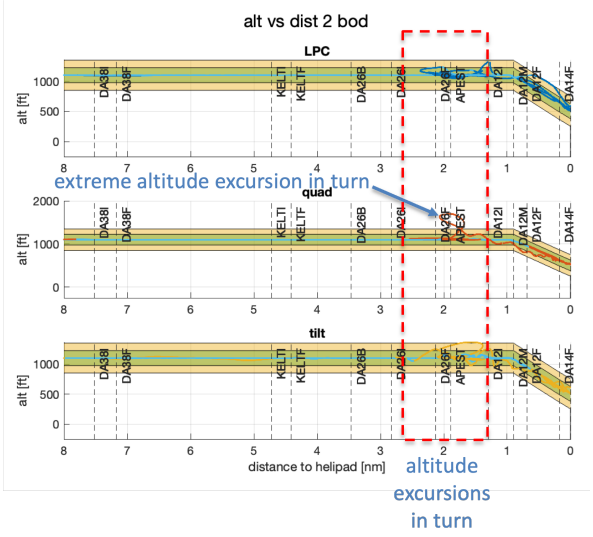
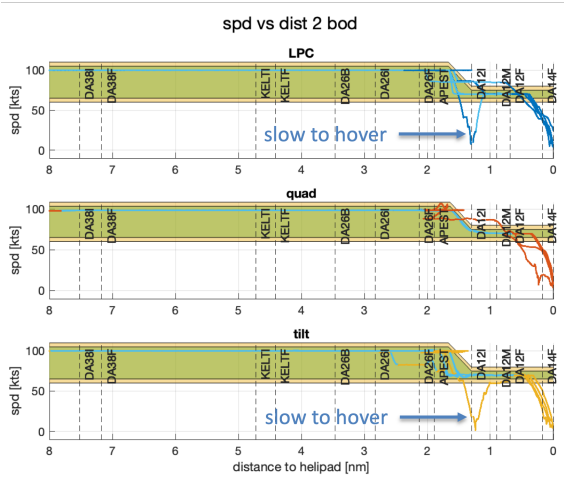


Fig. 29 Min distance from runway crossing during hold short



(a) altitude deviation vs distance to TD

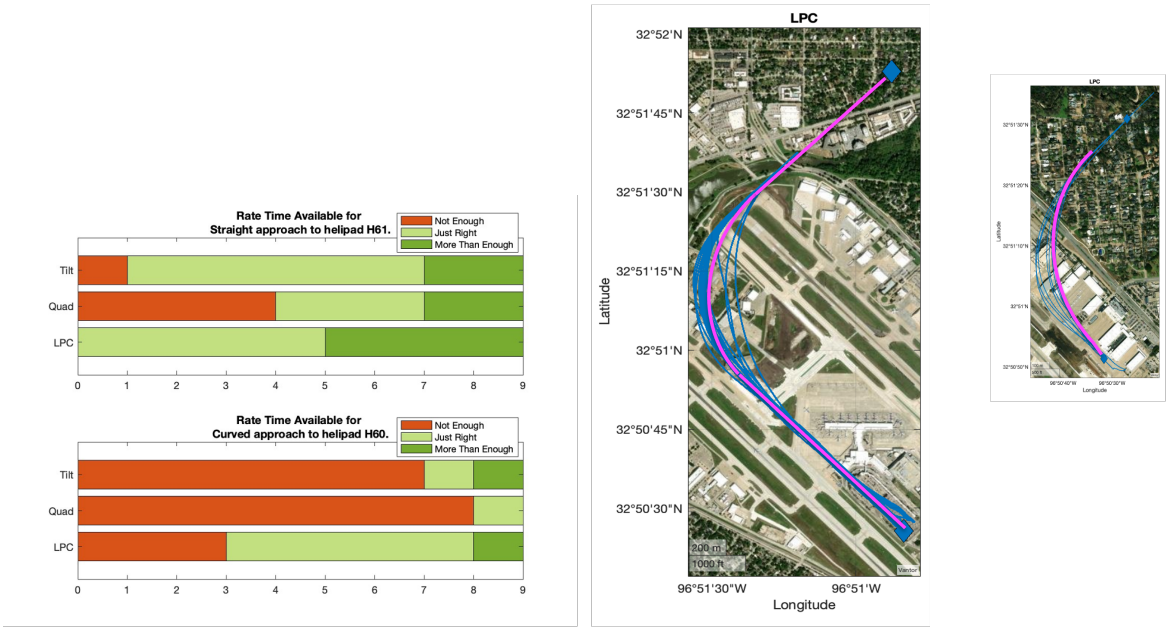


(b) speed deviation vs distance to TD

Fig. 30 Performance metrics in corridor for APEST runs with a hold short maneuver

C. Block 3: Approach and Landing

The approach and landing scenario compared a straight approach from APEST to DF61 and a curved approach from MDEST to DF60, as introduced in Fig. 17 in Sec. III.B.3. All pilots indicated concerns with the curved approach to DF60 in post-block surveys on procedure acceptance. The two main concerns, time pressure and overflying of aircraft, are demonstrated in Fig. 31. Comparing the time pressure as perceived by the pilots between the straight and curved approach in Fig. 31(a) shows that most pilots felt that they didn't have enough time to execute the curved approach, where generally the opposite was the case for the straight approach. Another observation is the contrast between the different vehicle designs. Both approach types show the similar trend that the quadcopter was the most demanding with respect to time pressure and the LPC the least, with the tilt somewhere in between both. It is notable that, for the LPC, all pilots agreed there was sufficient time on the straight approach. Moreover, the LPC had fewer pilots feeling rushed on the curved approach compared to the other vehicle designs. The lateral conformance was maintained in both the straight in and curved approaches depicted in Fig. 31(b). However, for the curved approach, zero runs were observed where the turn was cut short. Pilots commented on cutting the turn wide to avoid overflying parked aircraft and buildings in their post-simulation surveys. The contrast with the lateral performance of the straight in approach to DF61 is readily apparent in Fig. 31(b).



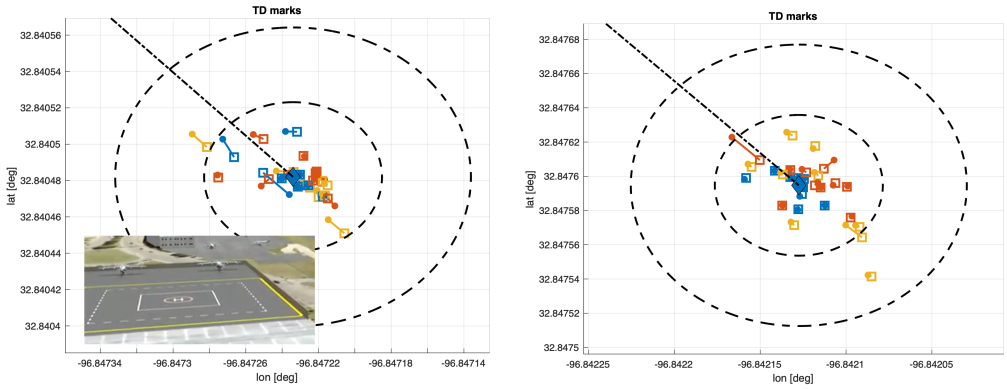
(a) Time pressure straight vs curved approach

(b) Ground tracks straight vs curved approach

Fig. 31 Metrics for final approach to DF60 and DF61

Figure 32 shows the location and remaining groundspeed at touchdown for the straight approaches to DF61 (Fig. 32(a)) and the curved approaches to DF60 (Fig. 32(b)). The radius of the inner circle is 15 ft and the outer circle is 30 ft. For each run at touchdown, the square and 'needle' marker indicate the location along with the direction and relative magnitude of the groundspeed vector. For both landing pads, most touchdowns were situated inside the inner circle with groundspeeds within tolerances. No distinctions between the different vehicle designs were observed. Comparing Fig. 32(a) and 32(b) shows that any groundspeed vector at touchdown for DF61 is either negligible or more likely pointing backwards against the direction of flight. This is most likely due to the parked vehicles immediately beyond the pad and the platform edge immediately behind them (pilot perspective just prior to touchdown is shown in inset in Fig. 32(a)). In addition, there is a potential loss of ground effect if the parking garage is overshot.

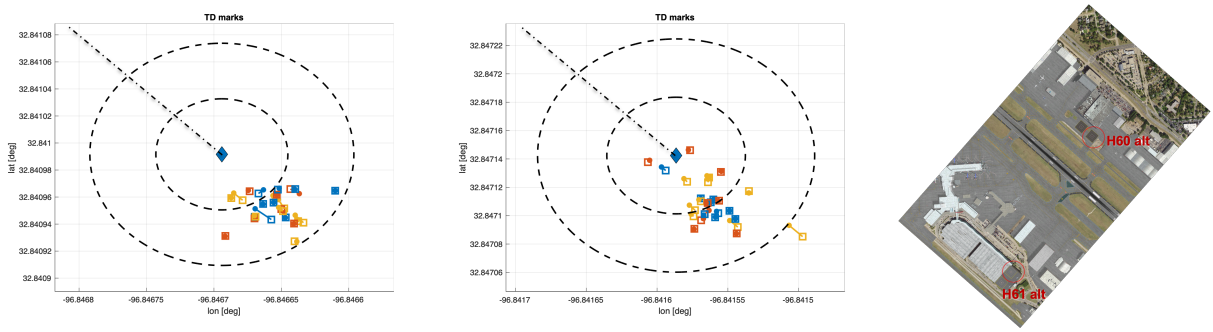
The Block 3 runs were randomized between either nominal or alternate pads for each approach. For half the runs, the pilots were required to land at the alternate pad in response to an ATC order given approximately 0.3 nm from the vertipad. For most runs, no significant impact was seen on the touchdown metrics despite the last-minute approach deviations. However, touchdown was often farther beyond the vertipad's center point demonstrated in Fig. 33. The



(a) Touchdown marks H61 (b) Touchdown marks H60

Fig. 32 Metrics for touchdown on H60 and H61 pads

reduced precision in touchdown points likely results from the lack of vertipad cues on the map display and PFD inset forcing pilots to rely solely on the out-the-window cuing. The lack of touchdown information for the alternate landing pads on the cockpit displays was twofold: (1.) no 'target' to time/place the groundspeed trend pointer when arming hover mode and (2.) less precision on the touchdown point. Note that one DF60 run in the tiltwing landed on the wrong pad (not shown in Fig. 33(b)) and one DF61 run in the quadcopter landed very early (not shown in Fig. 33(a)). No significant performance differences were observed comparing an alternate pad beyond the nominal one (Fig. 33(b)) with an alternate pad side-by-side with the nominal one (Fig. 33(a)). However, some pilots voiced concerns about overflying the nominal pad to reach the alternate pad (overshoots etc.). The relative positions of the alternate pads with respect to the nominal ones is shown in Fig. 33(c).

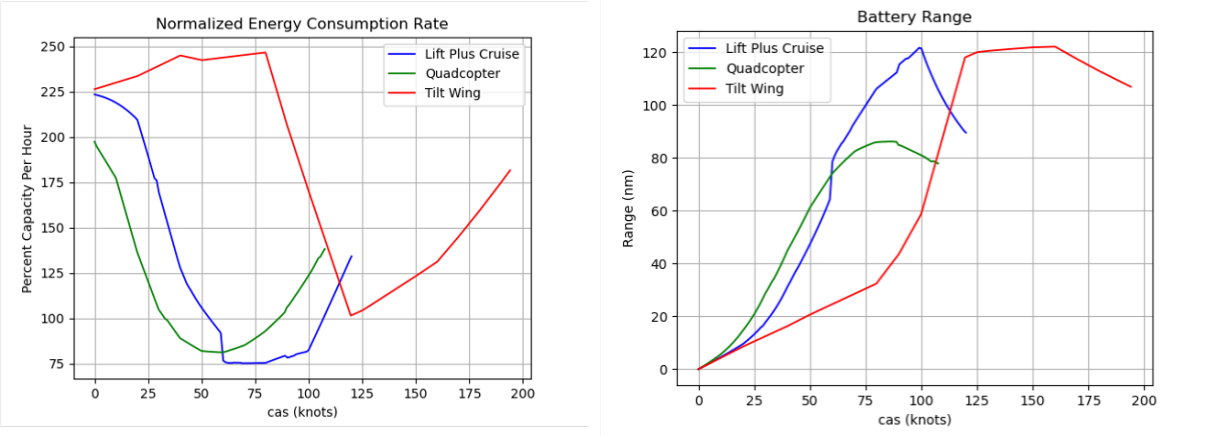


(a) Touchdown marks H61 alternate (b) Touchdown marks H60 alternate (c) Location of the alternate pads

Fig. 33 Metrics for touchdown on H60 and H61 alternate pads

D. Battery usage

Given the different performance envelopes of the three dissimilar vehicle designs, they also have very different battery usage profiles. Fig. 34 shows the differences between the three vehicle designs. The normalized energy consumption rate graph in Fig. 34(a) shows at which speed the maximum endurance (flight time) is achieved; while fig. 34(b) shows which speed results in the maximum range (distance flown). The quadcopter has better flight performance at lower speeds (max endurance at 60 kts, max range at 90 kts), the LPC does so in the intermediate speed range (max endurance at 80 kts and max range at 100 kts), and the tiltwing excels in the higher speed range (max endurance at 120 kts and max range at 160 kts).



(a) Normalized energy consumption rate

(b) Battery range

Fig. 34 Battery based performance specifications for the dissimilar aircraft designs

These battery usage profiles were implemented in the vehicle models used in this study, which allows for a comparative study of the battery usage among vehicles. The corridor scenario block with hold short is considered here since it allows comparing the three different approach transitions, as well as the impact of a slow down to hover maneuver to avoid crossing traffic. The results are presented in Fig. 35 which depicts the battery percentage used at the moment of touchdown as a function of flight time in minutes. The color coding of the markers indicates the different vehicles, with LPC in blue, quadcopter in red and tiltwing in amber. The different approach transitions are represented by the marker shapes, with circles for APEST, squares for MDEST and diamonds for MARSH. Filled markers are shown for left crosswind conditions and unfilled markers for right crosswind conditions.

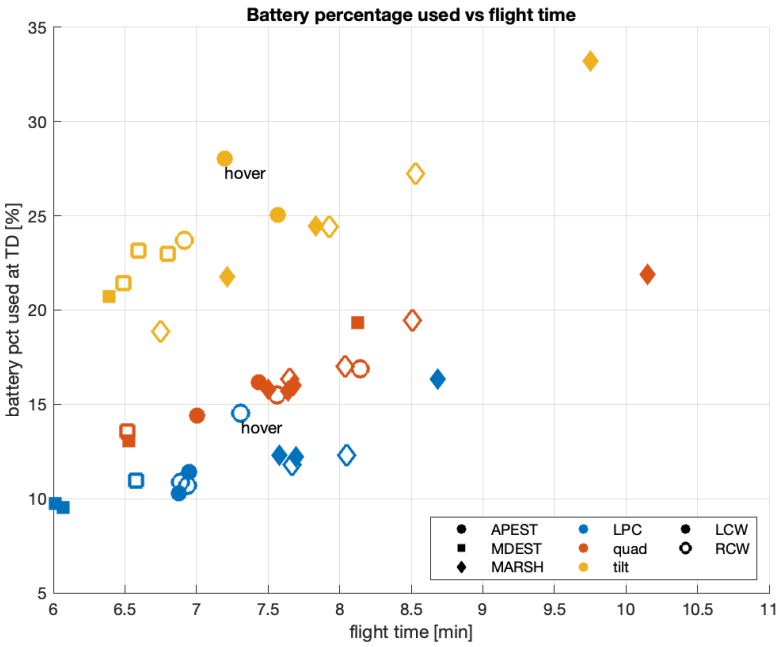
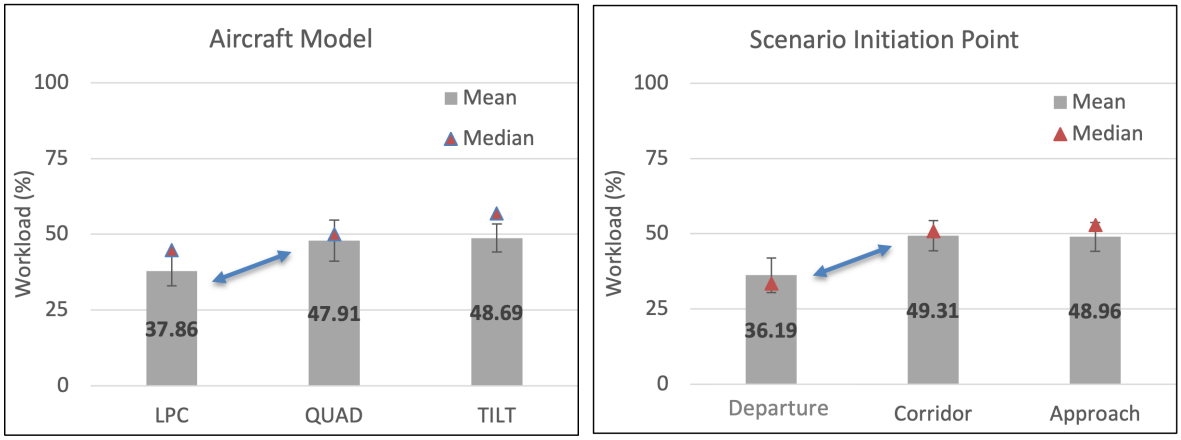


Fig. 35 Battery usage at touchdown per vehicle design and approach transition for the corridor scenario with hold short due to cross traffic

Overall trends in Fig. 35 show that the tiltwing has the highest battery usage percentage, followed by the quadcopter and the LPC has the lowest battery usage. This is consistent with trends in Fig. 34 at 100 kts calibrated airspeed which is the dominant speed value throughout these scenarios as can be seen in Fig. 30(b). Trends also indicate that MDEST approach transitions generally take a shorter time than APEST and MARSH generally takes the longest time. MARSH transitions also show the largest spread in flight times and battery usage. These differences in flight times reflect correspondingly in the battery usage numbers. No significant differences exist between left and right crosswind conditions. The two data points where one pilot slowed down to hover in APEST runs for the tiltwing and the LPC vehicles show a significant increase in battery usage because of the energy demanding extra hover time. Overall, the trends in Fig. 35 confirm expectations.

E. Workload

Workload was primarily assessed by means of the NASA workload TLX (See Ref. [20]) given in the cockpit via tablet after each run. Figure 36 provides a high level summary of the workload assessments across aircraft model Fig. 36(a)) and scenario (Fig. 36(b)). From the perspective of scenarios and flight phases, the departure and enroute scenario resulted in the lowest average workload. This is likely due to the higher autopilot usage resulting from both fewer contingencies and traffic conflicts as well as the exclusion of the approach and landing phase. In contrast, the workload ratings for the corridor scenarios were dominated by the landing task. For the curved approaches of Block 3, the alternate pad scenario resulted in a workload increase of only 3 – 5 %. With respect to aircraft models, the quadcopter and tiltwing show similar workload ratings, while the LPC yielded the lowest average workload. However, compared to the other vehicle designs, the challenging speed control of the tiltwing increased overall workload during curved approaches, hold short and slow quad scenarios.



(a) Differences based on aircraft model

(b) Differences based on scenario

Fig. 36 Workload metrics

In addition, Table 4 briefly illustrates the impact of pilot background on workload assessment. In particular, pilots with rotary-wing experience reported lower workload for all LPC and quadcopter runs as well as the tiltwing on final approach. One possible explanation is rotary-wing pilots are more accustomed to flying at lower speeds compared to fixed-wing pilots.

Table 4 Pilot workload versus experience

Rotorcraft experience	Average workload %
< 50% of total flight hrs	51%
≥ 50% of total flight hrs	29%

V. Summary

This simulator study evaluated proposed Urban Air Mobility (UAM) operations and procedure concepts to examine efficacy of the operations from the perspective of pilots flying. Scenarios were designed to explore new airspace operation concepts including interactions with mixed-equipage traffic including legacy transport traffic and other eVTOL traffic.

While it was found that RTA automation enabled pilots to achieve compliance with scheduled time of arrival (STA) at corridor entries with low workload; pilots would prefer to have clearance at the time of departure which may not be possible due to ATC workload and ability to predict ahead in time for longer flights. With automation, RNP-AR of 0.1 nm is achievable in corridors. However, when automation was not used, regardless of reason or intention, the ability to maintain the same RNP levels decreased. Multiple pilots commented on this difficulty stating: "For the RTA and width of those corridors I think the autopilot is required especially for this vehicle spacing" and "Definitely want autopilot, especially for single pilot." ATC frequency congestion was a concern for receiving both approach clearance and clearance to cross the runway, despite lower traffic conditions compared to what the pilot participants expected. The corridor arrival and straight in approaches to DF61 were acceptable for all vehicle designs; however, the curved approach to DF60 proved to be problematic with overflying aircraft and buildings and provided insufficient time on approach. Last but not least, hold short contingencies for crossing traffic are challenging and will need further development to be operationally feasible. They are time constrained and demanding in a complex and dense airspace, and result in a high workload task. Established procedures will be needed for incorporating delays that are usable across aircraft types. However, certain aircraft types and mixed-equipage can increase the workload for off-nominal events. For example, higher workloads occurred for the tiltwing when holding short or following a slower aircraft during corridor operations. There are two main observations with respect to workload. The primary drivers of the workload were performance as well as concerns about the visibility of surrounding traffic. Moreover, pilots with more rotary-wing experience reported significantly lower workload.

Finally, two main statements are given here as overall conclusions to this study. First, automation is necessary to achieve the required precision in the corridors. Secondly, airspace complexity and traffic density result in strict constraints that should be imposed on traffic. However, significantly different performance numbers of dissimilar vehicle designs require the necessary flexibility in these aforementioned constraints. This area of conflicting requirements imposed by airspace complexity and traffic density on one hand and vehicle performance dissimilarity on the other warrants further investigation to inform the future development of xTM airspace operations.

Acknowledgment

This study was funded by NASA's Airspace Operations and Safety Program's (AOSP) Air Mobility Pathfinder (AMP) project. The authors would like to thank the NASA Ames Vertical Motion Simulator (VMS) staff Matt Blanken, Sam Orth and Peter Zaal for supporting this experiment.

Appendix: AEP-3 Vehicle Model Differences: Vehicle Control Configuration

Figure 37 shows the different vehicle control configurations for the three dissimilar vehicle designs. The quadcopter, LPC and tiltwing have fundamentally different strategies to control vertical motion and speed by means of pitch and heave, depending on the flight mode. For example, speed is controlled by pitch in the quadrotor and when the tiltwing is in thrust borne lift mode. However, speed is controlled by thrust in the semi-wing and wing-borne modes for the tiltwing and in the LPC in all flight modes.

Flight Regime		Quadcopter 	LPC 	Tiltwing 
Vehicle Class		eVTOL	Winged eVTOL	Winged eVTOL
Number of Active Control Axes		4	5	4
Vertical Control	Thrust Borne Lift	Heave for climb/descent	Heave for climb/descent	Heave from climb/descent
	Semi Wing Borne & Wing Borne Lift		Pitch for climb/descent	Pitch for climb/descent
Acceleration Control	Thrust Borne Lift	Speed on pitch	Speed on thrust	Speed on pitch
	Semi Wing Borne & Wing Borne Lift			Speed on thrust

Fig. 37 AEP-3 Vehicle Model Differences: Vehicle Control Configuration

References

[1] (FAA), F. A. A., "Urban Air Mobility (UAM) Concept of Operations, V2," Tech. rep., Federal Aviation Administration (FAA), Washington, DC, 2023. URL `https://www.faa.gov/air-taxis/uam_blueprint`.

[2] Verma, S., Mogford, R., Shyr, M., Farrahi, A., Wood, R., Torres, G., Keeler, J., Mueller, E., Bosson, C., Prevot, T., and Ghatas, R., "Evaluation of Initial and Mid-Term Air Traffic Procedures for Urban Air Mobility Operations," *AIAA AVIATION FORUM AND ASCEND 2024*, American Institute of Aeronautics and Astronautics, 2024. doi:10.2514/6.2024-4455.

[3] Verma, S., Keeler, J., Shyr, M., Rosado, G., Mogford, R., Mueller, E., Prevot, T., Bosson, C., Ghatas, R., Farrahi, A., and Wood, R., "Evaluation of Initial and Midterm Air Traffic Procedures for Urban Air Mobility Operations," techreport NASA/TM-20240012776, NASA, Moffett Field, CA, USA, 2024. URL `https://ntrs.nasa.gov/api/citations/20240012776/downloads/NASA-TM-2024001776.pdf`.

[4] Lee, H., Lee, A., Guillermo, L., Seah, C., and Moolchandani, K. A., "Simulated Evaluation of Strategic Conflict Management Capabilities for Urban Air Mobility Operations," *AIAA AVIATION FORUM AND ASCEND 2024*, American Institute of Aeronautics and Astronautics, 2024. doi:DOI: 10.2514/6.2024-3854.

[5] Lee, H., Lee, A., Seah, C. H., Lee, C. H., and Moolchandani, K., "Provider of Services for Urban Air Mobility (PSU) Prototype Simulation (X5) Final Report," techreport NASA/TM-20250001367, NASA, Moffett Field, CA, USA, Feb. 2025. URL `https://ntrs.nasa.gov/api/citations/20250001367/downloads/NASA-TM-20250001367.pdf`.

[6] Magyarits, S., "Extensible Traffic Management (xTM)," techreport, FAA, 2022. URL `https://www.faa.gov/sites/faa.gov/files/2022-03/508.05Spring2022REDACNASOps_XTM.pdf`.

[7] Kaneshige, J., Lombaerts, T., Shish, K., and Feary, M., "Command and Control Concepts for a Lift Plus Cruise Electric Vertical Takeoff and Landing Vehicle," *AIAA AVIATION 2023 FORUM*, American Institute of Aeronautics and Astronautics, 2023. doi:10.2514/6.2023-3910.

[8] Kaneshige, J., Lombaerts, T., Shish, K., and Feary, M., "Simplified Vehicle Control Concept for a Lift Plus Cruise eVTOL Vehicle," *AIAA AVIATION FORUM AND ASCEND 2024*, American Institute of Aeronautics and Astronautics, 2024. doi:10.2514/6.2024-4207.

[9] Lombaerts, T., Shish, K., Kaneshige, J., Villa, A., Feary, M., Monk, K., Haworth, L., Steglinski, M., Kurklu, E., Iwai, N., and Archdeacon, J., "Simulator Evaluations of Assistive Hover Automation Concepts for a Lift Plus Cruise eVTOL Vehicle," *IEEE Digital Avionics Systems Conference 2025*, IEEE, 2025. doi:10.1109/DASC66011.2025.11257285.

[10] Silva, C., Johnson, W. R., Solis, E., Patterson, M. D., and Antcliff, K. R., "VTOL Urban Air Mobility Concept Vehicles for Technology Development," *2018 ATIO Conference*, AIAA, 2018. doi:10.2514/6.2018-3847.

[11] Whiteside, S., Pollard, B., Antcliff, K., Zawodny, A., Fei, X., Silva, C., and Medina, G., "Design of a Tiltwing Concept Vehicle for Urban Air Mobility," techreport NASA/TM-20210017971, NASA, Moffett Field, CA, USA, 2021. URL https://ntrs.nasa.gov/api/citations/20210017971/downloads/NASA-TM-20210017971.pdf.

[12] "Approval Guidance for Required Navigation Performance (RNP) Procedures with Authorization Required (AR) Including Change 1," Advisory Circular AC90-101A, FAA, 2011. URL https://www.faa.gov/documentLibrary/media/Advisory_Circular/AC_90-101A_CHG_1.pdf.

[13] Lombaerts, T., Kaneshige, J., and Feary, M., "Control Concepts for Simplified Vehicle Operations of a Quadrotor eVTOL Vehicle," *AIAA AVIATION 2020 FORUM*, American Institute of Aeronautics and Astronautics, 2020. doi:10.2514/6.2020-3189.

[14] Nicholas, O. P., and Bennett, P. J., "Proposed Wide Envelope Unified Control Concept for Vectored Thrust VSTOL Aircraft," Technical Memorandum FS312, Royal Aircraft Establishment RAE, Mar. 1980.

[15] Meyer, G., and Cicolani, L., "A Formal Structure for Advanced Automatic Flight Control Systems," techreport NASA TN D-7940, NASA, May 1975. URL https://ntrs.nasa.gov/archive/nasa/casi.ntrs.nasa.gov/19750015534.pdf.

[16] De Smedt, D., and Berz, G., "Study of the required time of arrival function of current FMS in an ATM context," *IEEE Digital Avionics Systems Conference 2007*, IEEE, 2007. doi:10.1109/DASC.2007.4391837.

[17] Danek, G., "Vertical motion simulator familiarization guide," Technical report NASA-TM-103923, NASA Ames Research Center, May 1993. URL https://ntrs.nasa.gov/search.jsp?R=19940008535.

[18] Beard, S., Reardon, S., Tobias, E., and Aponso, B., "Simulation System Optimization for Rotorcraft Research on the Vertical Motion Simulator Read More: https://arc.aiaa.org/doi/abs/10.2514/6.2012-4634," *AIAA Modeling and Simulation Technologies Conference*, AIAA 2012-4634, American Institute of Aeronautics and Astronautics, 2012. doi:10.2514/6.2012-4634.

[19] Lewis, E., and Vuong, N., "Integration of Matlab Simulink Models with the Vertical Motion Simulator," *AIAA Modeling and Simulation Technologies Conference*, American Institute of Aeronautics and Astronautics, 2012. doi:10.2514/6.2012-4797.

[20] Hart, S. G., and Staveland, L. E., *Human Mental Workload*, Amsterdam: North Holland Press, 1988, Chaps. Development of NASA-TLX (Task Load Index): Results of Empirical and Theoretical Research. doi:10.1016/s0166-4115(08)62386-9.